

Global Momentum Compression for Sparse Communication in Distributed Learning

Chang-Wei Shi[†]

Shen-Yi Zhao[†]

Yin-Peng Xie

Hao Gao

Wu-Jun Li^{*}

SHICW@SMAIL.NJU.EDU.CN

ZHAOSY1009@GMAIL.COM

2418111594@QQ.COM

GH131220003@GMAIL.COM

LIWUJUN@NJU.EDU.CN

National Key Laboratory for Novel Software Technology

Department of Computer Science and Technology

Nanjing University, Nanjing 210023, China

Abstract

With the rapid growth of data, distributed momentum stochastic gradient descent (DMSGD) has been widely used in distributed learning, especially for training large-scale deep models. Due to the latency and limited bandwidth of the network, communication has become the bottleneck of distributed learning. Communication compression with sparsified gradient, abbreviated as *sparse communication*, has been widely employed to reduce communication cost. All existing works about sparse communication in DMSGD employ local momentum, in which the momentum only accumulates stochastic gradients computed by each worker locally. In this paper, we propose a novel method, called *global momentum compression* (GMC), for sparse communication. Different from existing works that utilize local momentum, GMC utilizes global momentum. Furthermore, to enhance the convergence performance when using more aggressive sparsification compressors (e.g., RBGS), we extend GMC to GMC+. We theoretically prove the convergence of GMC and GMC+. To the best of our knowledge, this is the first work that introduces global momentum for sparse communication in distributed learning. Empirical results demonstrate that, compared with the local momentum counterparts, our GMC and GMC+ can achieve higher test accuracy and exhibit faster convergence, especially under non-IID data distribution.

Keywords: sparse communication, momentum, distributed machine learning, stochastic gradient descent, error feedback

1 Introduction

Many machine learning models can be formulated as the following empirical risk minimization problem:

$$\min_{\mathbf{w} \in \mathbb{R}^d} F(\mathbf{w}) = \frac{1}{|\mathcal{D}|} \sum_{\xi \in \mathcal{D}} f(\mathbf{w}; \xi), \quad (1)$$

where \mathbf{w} denotes the model parameter of dimension d , \mathcal{D} denotes the training dataset, $f(\mathbf{w}; \xi)$ is the empirical loss on the instance ξ , $|\mathcal{D}|$ is the number of training instances. For example, let $\xi = (\mathbf{x}, y)$, where \mathbf{x} denotes the feature of the training data and y denotes the

[†]. Equal contribution.

^{*}. Corresponding author.

label. Then in logistic regression $f(\mathbf{w}; \xi) = \log(1 + e^{-y\mathbf{x}^T\mathbf{w}}) + \frac{\lambda}{2}\|\mathbf{w}\|^2$, and in support vector machine (SVM) $f(\mathbf{w}; \xi) = \max(0, 1 - y\mathbf{x}^T\mathbf{w}) + \frac{\lambda}{2}\|\mathbf{w}\|^2$. Many deep learning models can also be formulated as (1).

Stochastic gradient descent (SGD) and its variants (Robbins and Monro, 1951; Bottou, 2010; Johnson and Zhang, 2013; Zhao et al., 2018, 2020, 2021) have been the dominating optimization methods for solving (1). In each iteration, SGD calculates a (mini-batch) stochastic gradient and uses it to update the model parameters. Inspired by momentum and Nesterov’s accelerated gradient descent, momentum SGD (MSGD) (Polyak, 1964; Tseng, 1998; Lan, 2012; Kingma and Ba, 2015) has been proposed and widely used in machine learning. In practice, MSGD often outperforms SGD (Krizhevsky et al., 2012; Sutskever et al., 2013). Many machine learning platforms, such as TensorFlow, PyTorch and MXNet, include MSGD as one of their optimization methods.

With the rapid growth of data, distributed SGD (DSGD) and its variant distributed MSGD (DMSGD) have garnered much attention. They distribute the stochastic gradient computation across multiple workers to expedite the model training. These methods can be implemented on distributed frameworks like parameter server and all-reduce frameworks. Each worker computes stochastic gradients locally and communicates with the server or other workers to obtain the aggregated stochastic gradients for updating the model parameter. Recently, more and more large-scale deep learning models, such as large language models (Devlin et al., 2019; Brown et al., 2020; Touvron et al., 2023), have been proposed in machine learning. In large-scale model training tasks, the communicated messages become high-dimensional vectors. Due to the latency and limited bandwidth of the network, communication cost has become the bottleneck of distributed learning, especially for cases with large-scale models. To address the communication bottleneck issue, there have been many works dedicated to compressing the communicated messages (Wen et al., 2017; Alistarh et al., 2017; Aji and Heafield, 2017; Jiang and Agrawal, 2018; Alistarh et al., 2018; Stich et al., 2018; Lin et al., 2018; Vogels et al., 2019; Karimireddy et al., 2019; Tang et al., 2019; Xie et al., 2020; Xu and Huang, 2022).

Researchers have proposed two main categories of communication compression methods for reducing communication cost: quantization (Wen et al., 2017; Alistarh et al., 2017; Jiang and Agrawal, 2018) and sparsification (Aji and Heafield, 2017; Alistarh et al., 2018; Stich et al., 2018; Karimireddy et al., 2019; Tang et al., 2019). Quantization methods quantize the value (gradient or parameter) representation from float (typically 32 bits) to lower bit-width, such as eight bits or four bits. It’s easy to find that the communication cost can be reduced at most by 31-fold in the ideal case. Sparsification methods, which are also called *sparse communication* methods, select only a few components of the vector for communicating with the server or the other workers. The most widely used sparsification compressor adopted in sparse communication methods is top- s , where each worker selects s components of the vector with the largest absolute values. Considering the high-dimensional nature of communicated vectors in large-scale model training, sparsification methods have the potential to achieve a much higher level of communication compression compared to the maximum 31-fold compression achieved by quantization methods.

Due to the presence of compressed error, naively compressing the communicated vectors in DSGD or DMSGD will damage the convergence, especially when the compression ratio is high. The most representative technique designed to tackle this issue is error feed-

back (Stich et al., 2018; Karimireddy et al., 2019), also called error compensation or memory vector. The error feedback technique keeps the compressed error into the error residual on each worker and incorporates the error residual into the next update. Error feedback based sparse communication methods have been widely adopted by recent communication compression methods and achieved better performance than quantization methods and other sparse communication methods without error feedback. In existing error feedback based sparse communication methods, most are for vanilla DSGD (Aji and Heafield, 2017; Alistarh et al., 2018; Stich et al., 2018; Karimireddy et al., 2019; Tang et al., 2019). There has appeared one error feedback based sparse communication method for DMSGD, called Deep Gradient Compression (DGC) (Lin et al., 2018), which has achieved better performance than vanilla DSGD with sparse communication in practice. However, the theory about the convergence of DGC is still lacking. Furthermore, although DGC combines momentum and error feedback, the momentum in DGC only accumulates stochastic gradients computed by each worker locally. Therefore, the momentum in DGC is a local momentum without global information.

Recently, Xie et al. (2020) proposes Communication-efficient SGD with Error Reset (CSER) that combines partial synchronization and error reset techniques. Due to the extra communication and computation overhead of the top- s compressor, some works (Vogels et al., 2019; Xie et al., 2020; Xu and Huang, 2022) also consider a more aggressive sparsification compressor, called Random Blockwise Gradient Sparsification (RBGS). Since RBGS introduces a larger compressed error compared with top- s when selecting the same number of components of the original vector to communicate, vanilla error feedback methods usually fail to converge when using RBGS as the sparsification compressor. To address this convergence issue, Xu and Huang (2022) proposes DEF-A, which utilizes the detached error feedback technique. Both CSER and DEF-A have their momentum variants (Xie et al., 2020; Xu and Huang, 2022), but they use local momentum similar to DGC.

In this paper, we introduce global momentum and propose a novel method, called global momentum compression (GMC), for sparse communication in distributed learning based on error feedback. The main contributions of this paper are outlined as follows:

- GMC combines error feedback and momentum to achieve sparse communication in distributed learning. But different from existing sparse communication methods like DGC which adopt local momentum, GMC adopts global momentum. To the best of our knowledge, this is the first work to introduce global momentum into sparse communication methods.
- Furthermore, to enhance the convergence performance when using more aggressive sparsification compressors (e.g., RBGS), we extend GMC to GMC+ by introducing global momentum to the detached error feedback technique.
- We theoretically prove the convergence of both GMC and GMC+.
- Empirical results demonstrate that, compared with the local momentum counterparts, GMC and GMC+ can achieve higher test accuracy and exhibit faster convergence, especially under non-IID data distribution.

2 Preliminary

2.1 Notations

In this paper, we use $\|\cdot\|$ to denote L_2 norm and use $\mathcal{C}(\cdot)$ to denote the sparsification compressor. For $n \in \mathbb{N}_+$, we use $[n]$ to denote $\{0, 1, 2, \dots, n-1\}$. $\nabla f(\mathbf{w}; \mathcal{I}) \triangleq \frac{1}{|\mathcal{I}|} \sum_{\xi \in \mathcal{I}} \nabla f(\mathbf{w}; \xi)$ denotes one stochastic gradient with respect to a mini-batch of training instances \mathcal{I} . For a vector \mathbf{a} , we use $a^{(j)}$ to denote its j -th component. $\|\mathbf{a}\|_0$ denotes the number of non-zero components in \mathbf{a} .

2.2 Problem Formulation

Assume we have K workers. The training data are distributed or partitioned across K workers. Let \mathcal{D}_k denote the training data stored on worker k , and $F_k(\mathbf{w}) = \frac{1}{|\mathcal{D}_k|} \sum_{\xi \in \mathcal{D}_k} f(\mathbf{w}; \xi)$ denote the local objective function on worker k . Assume $\mathcal{D}_k \cap \mathcal{D}_{k'} = \emptyset$ if $k \neq k'$, it's easy to verify that $F(\mathbf{w}) = \frac{1}{|\mathcal{D}|} \sum_{\xi \in \mathcal{D}} f(\mathbf{w}; \xi) = \sum_{k \in [K]} \frac{|\mathcal{D}_k|}{|\mathcal{D}|} F_k(\mathbf{w})$, where $\mathcal{D} = \cup_{k=1}^K \mathcal{D}_k$. Without loss of generality, we assume that each worker has the same number of training data, that is $|\mathcal{D}_k| = |\mathcal{D}_{k'}|, \forall k, k' \in [K]$. Then the problem in (1) can be rewritten as

$$\min_{\mathbf{w} \in \mathbb{R}^d} F(\mathbf{w}) = \frac{1}{K} \sum_{k \in [K]} F_k(\mathbf{w}). \quad (2)$$

2.3 Distributed Momentum SGD

The widely used momentum SGD (MSGD) (Polyak, 1964) can be written as

$$\begin{aligned} \mathbf{m}_{t+1} &= \beta \mathbf{m}_t + \eta \nabla f(\mathbf{w}_t; \mathcal{I}_t), \\ \mathbf{w}_{t+1} &= \mathbf{w}_t - \mathbf{m}_{t+1}, \end{aligned}$$

where $\beta \in [0, 1]$. \mathbf{m}_t is the Polyak's momentum. $\nabla f(\mathbf{w}_t; \mathcal{I}_t)$ is one stochastic gradient with respect to a mini-batch of training instances \mathcal{I}_t sampled from \mathcal{D} . Since $\mathbf{m}_t = -(\mathbf{w}_t - \mathbf{w}_{t-1})$, MSGD can also be written as

$$\mathbf{w}_{t+1} = \mathbf{w}_t - \eta (\nabla f(\mathbf{w}_t; \mathcal{I}_t) - \frac{\beta}{\eta} (\mathbf{w}_t - \mathbf{w}_{t-1})). \quad (3)$$

Please note that if $\beta = 0$, MSGD degenerates to SGD.

One way to implement distributed MSGD (DMSGD) is using *local momentum*:

$$\mathbf{m}_{t+1,k} = \beta \mathbf{m}_{t,k} + \eta \nabla f(\mathbf{w}_t; \mathcal{I}_{t,k}), |\mathcal{I}_{t,k}| = b, k \in [K], \quad (4)$$

$$\mathbf{w}_{t+1} = \mathbf{w}_t - \frac{1}{K} \sum_{k \in [K]} \mathbf{m}_{t+1,k}, \quad (5)$$

where $\mathbf{m}_{0,k} = \mathbf{0}, k \in [K]$ and $\nabla f(\mathbf{w}_t; \mathcal{I}_{t,k})$ is the stochastic gradient with respect to a mini-batch $\mathcal{I}_{t,k}$ of size b sampled from \mathcal{D}_k on worker k . This update process can be rewritten as

$$\mathbf{w}_{t+1} = \mathbf{w}_t - \frac{1}{K} \sum_{k \in [K]} \mathbf{m}_{t+1,k} = \mathbf{w}_t - \frac{\eta}{K} \sum_{k \in [K]} \nabla f(\mathbf{w}_t; \mathcal{I}_{t,k}) - \frac{\beta}{K} \sum_{k \in [K]} \mathbf{m}_{t,k}. \quad (6)$$

Since $\frac{1}{K} \sum_{k \in [K]} \mathbf{m}_{t,k} = -(\mathbf{w}_t - \mathbf{w}_{t-1})$ and $\frac{1}{K} \sum_{k \in [K]} \nabla f(\mathbf{w}_t; \mathcal{I}_{t,k}) = \nabla f(\mathbf{w}_t; \mathcal{I}_t)$, $\mathcal{I}_t = \cup_{k \in [K]} \mathcal{I}_{t,k}$, this implementation of DMSGD is equivalent to the serial MSGD in (3). $\mathbf{m}_{t,k}, k \in [K]$ is called *local momentum* since it only accumulates local gradient information from worker k .

Another way to implement DMSGD is that each worker parallelly computes some stochastic gradients and then the stochastic gradients of all workers are aggregated to get $\nabla f(\mathbf{w}_t; \mathcal{I}_t) - \beta(\mathbf{w}_t - \mathbf{w}_{t-1})/\eta$ in (3). The update process of \mathbf{w} in this way is equivalent to the serial MSGD. We call $-(\mathbf{w}_t - \mathbf{w}_{t-1})/\eta$ the *global momentum*, because it captures the global gradient information from all workers.

We can find that both local momentum and global momentum implementations of DMSGD are equivalent to the serial MSGD if no sparse communication is adopted. However, when it comes to adopting sparse communication, things become different. In the later sections, we will demonstrate that global momentum is better than local momentum when implementing sparse communication in DMSGD.

3 Global Momentum Compression

Our method global momentum compression (GMC) mainly performs the following operations iteratively:

- Each worker computes $\nabla f(\mathbf{w}_t; \mathcal{I}_{t,k}) = \frac{1}{b} \sum_{\xi \in \mathcal{I}_{t,k}} \nabla f(\mathbf{w}_t; \xi)$, where $\mathcal{I}_{t,k}$ is a mini-batch randomly sampled from \mathcal{D}_k and $|\mathcal{I}_{t,k}| = b$;
- Each worker computes $\mathbf{e}_{t+\frac{1}{2},k} = \mathbf{e}_{t,k} + \nabla f(\mathbf{w}_t; \mathcal{I}_{t,k}) - \frac{\beta}{\eta}(\mathbf{w}_t - \mathbf{w}_{t-1})$, and then sends the sparsified vector $\mathcal{C}(\mathbf{e}_{t+\frac{1}{2},k})$ to the server or other workers;
- Each worker updates the error residual $\mathbf{e}_{t+1,k} = \mathbf{e}_{t+\frac{1}{2},k} - \mathcal{C}(\mathbf{e}_{t+\frac{1}{2},k})$;
- Update parameter $\mathbf{w}_{t+1} = \mathbf{w}_t - \frac{\eta}{K} \sum_{k \in [K]} \mathcal{C}(\mathbf{e}_{t+\frac{1}{2},k})$.

3.1 Framework of GMC

GMC can be easily implemented on the all-reduce distributed framework in which each worker sends the sparsified vector $\mathcal{C}(\mathbf{e}_{t+\frac{1}{2},k})$ to all the other workers, then each worker updates \mathbf{w}_{t+1} after receiving the sparsified vectors from all the other workers.

Recently, parameter server (Li et al., 2014) has been one of the most popular distributed frameworks in machine learning. GMC can also be implemented on the parameter server framework. In this paper, we adopt the parameter server framework for illustration. The theories in this paper can also be adapted for the all-reduce framework. The details of GMC implemented on the parameter server framework are shown in Algorithm 1. After updating \mathbf{w}_{t+1} , the server in GMC will send $\mathbf{w}_{t+1} - \mathbf{w}_t$, rather than \mathbf{w}_{t+1} , to workers. Since $\mathcal{C}(\mathbf{e}_{t+\frac{1}{2},k})$ is sparse, $\mathbf{w}_{t+1} - \mathbf{w}_t$ is sparse as well. Hence, sending $\mathbf{w}_{t+1} - \mathbf{w}_t$ can reduce the communication cost compared with sending \mathbf{w}_t . Workers can get \mathbf{w}_{t+1} by $\mathbf{w}_{t+1} = \mathbf{w}_t + (\mathbf{w}_{t+1} - \mathbf{w}_t)$.

Remark 1 *There are some other ways to combine momentum and error feedback. For example, we can put the momentum term on the server. However, these ways lead to*

Algorithm 1 GMC

```

1: Input: sparsification compressor  $\mathcal{C}(\cdot)$ , number of workers  $K$ , number of iterations  $T$ ,
   model parameters  $\mathbf{w}_0$ , learning rate  $\eta$ , momentum coefficient  $\beta \in [0, 1)$ , training dataset
    $\mathcal{D}_k, \forall k \in [K]$ ;
2: Set  $\mathbf{w}_{-1} = \mathbf{w}_0, \mathbf{e}_{0,k} = \mathbf{0}, \forall k \in [K]$ ;
3: for iteration  $t \in [T]$  do
4:   Workers:
5:   for worker  $k \in [K]$  parallelly do
6:     Randomly pick a mini-batch of training data  $\mathcal{I}_{t,k} \subseteq \mathcal{D}_k$  with  $|\mathcal{I}_{t,k}| = b$  and compute
        $\nabla f(\mathbf{w}_t; \mathcal{I}_{t,k}) = \frac{1}{b} \sum_{\xi \in \mathcal{I}_{t,k}} \nabla f(\mathbf{w}_t; \xi)$ ;
7:      $\mathbf{e}_{t+\frac{1}{2},k} = \mathbf{e}_{t,k} + \nabla f(\mathbf{w}_t; \mathcal{I}_{t,k}) - \frac{\beta}{\eta}(\mathbf{w}_t - \mathbf{w}_{t-1})$ ;
8:     Generate a sparse vector  $\mathcal{C}(\mathbf{e}_{t+\frac{1}{2},k})$  and send  $\mathcal{C}(\mathbf{e}_{t+\frac{1}{2},k})$  to the server;
9:     Update the error residual  $\mathbf{e}_{t+1,k} = \mathbf{e}_{t+\frac{1}{2},k} - \mathcal{C}(\mathbf{e}_{t+\frac{1}{2},k})$ ;
10:    Receive  $\mathbf{w}_{t+1} - \mathbf{w}_t$  from server;
11:    Get  $\mathbf{w}_{t+1}$  by  $\mathbf{w}_{t+1} = \mathbf{w}_t + (\mathbf{w}_{t+1} - \mathbf{w}_t)$ ;
12:   end for
13:   Server:
14:   Receive  $\mathcal{C}(\mathbf{e}_{t+\frac{1}{2},k})$  from all the workers;
15:    $\mathbf{w}_{t+1} = \mathbf{w}_t - \eta \frac{1}{K} \sum_{k \in [K]} \mathcal{C}(\mathbf{e}_{t+\frac{1}{2},k})$ ;
16:   Send  $\mathbf{w}_{t+1} - \mathbf{w}_t$  to workers;
17: end for

```

worse performance than the way adopted in this paper. More discussions can be found in Appendix A.

We can find that DGC (Lin et al., 2018) is mainly based on the local momentum while GMC is based on the global momentum. Hence, each worker in DGC cannot capture the global information from its local momentum, while that in GMC can capture the global information from the global momentum even if sparse communication is adopted.

Remark 2 We find that due to the momentum factor masking (mfm) in DGC (Lin et al., 2018), DGC (w/ mfm) will degenerate to DSGD rather than DMSGD if sparse communication is not adopted, while GMC will degenerate to DMSGD if sparse communication is not adopted. To make a comprehensive comparison of these methods, we will compare GMC with two implementations of DGC: DGC (w/ mfm) and DGC (w/o mfm). Different from DGC (w/ mfm), DGC (w/o mfm) will degenerate to DMSGD if sparse communication is not adopted.

3.2 Benefit of Global Momentum

To illustrate the benefit of global momentum for sparse communication, we investigate the convergence behavior of these methods when minimizing a simple quadratic objective function $F(\mathbf{w})$. Let $n = K = 2$, $\mathbf{w} = (w^{(0)}, w^{(1)}, \dots, w^{(d-1)})^T \in \mathbb{R}^d$, $\mathcal{D} = \{\xi_1, \xi_2\}$, $\mathcal{D}_1 =$

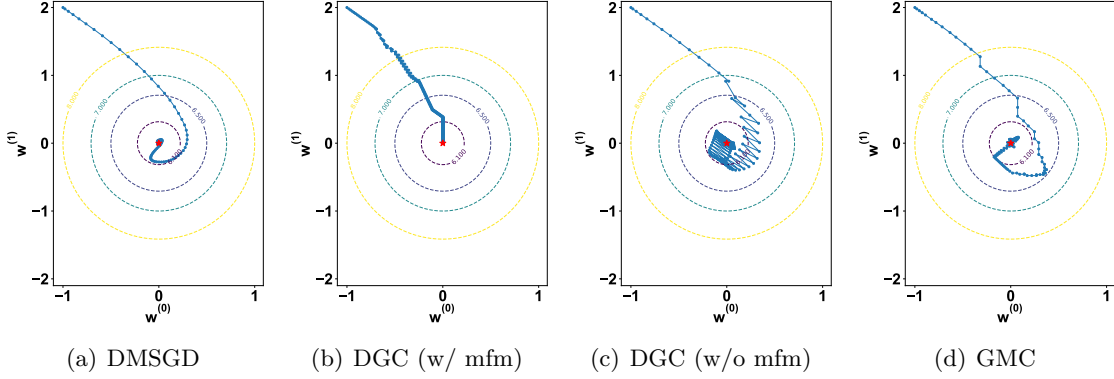


Figure 1: Comparison of optimization trajectories of different methods.

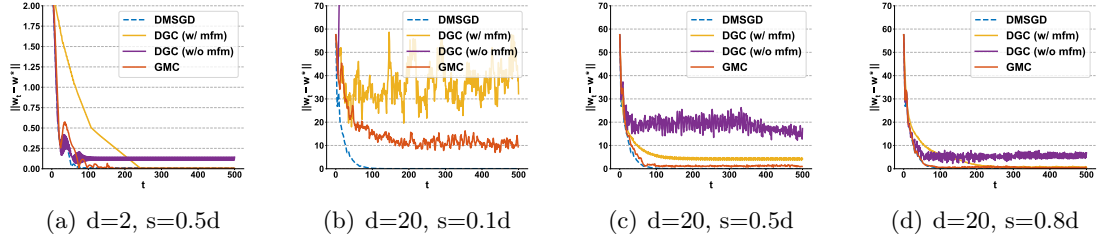


Figure 2: Comparison of the distances to the global optimal point of different methods.

$\{\xi_1\}, \mathcal{D}_2 = \{\xi_2\}$, we define the objective functions as follows:

$$\begin{aligned}
 F_0(\mathbf{w}) &= f(\mathbf{w}; \xi_1) = \sum_{i \in [d]} (d - i) * [w^{(i)} - (i + 1)]^2, \\
 F_1(\mathbf{w}) &= f(\mathbf{w}; \xi_2) = \sum_{i \in [d]} (d - i) * [w^{(i)} + (i + 1)]^2, \\
 F(\mathbf{w}) &= \frac{1}{2}(F_0(\mathbf{w}) + F_1(\mathbf{w})) = \sum_{i \in [d]} (d - i) * [(w^{(i)})^2 + (i + 1)^2].
 \end{aligned}$$

It's easy to verify that the global optimal point to minimize $F(\mathbf{w})$ is $\mathbf{w}^* = (0, 0, \dots, 0)^T \in \mathbb{R}^d$. The optimal point to minimize local objective function $F_0(\mathbf{w})$ is $(1, 2, \dots, d)^T$, while it's $(-1, -2, \dots, -d)^T$ for $F_1(\mathbf{w})$. We run DMSGD, DGC (w/ mfm), DGC (w/o mfm) and GMC respectively to solve the optimization problem: $\min_{\mathbf{w} \in \mathbb{R}^d} F(\mathbf{w})$. The momentum coefficient β is set as 0.9 and the learning rate is set as 0.005. We use top- s as the sparsification compressor.

Firstly, we set $d = 2$ and the optimization trajectories of different methods starting from the point $(-1, 2)$ are shown in Figure 1. We can find that after a sufficient number of iterations, the parameter in DGC (w/o mfm) can only oscillate within a relatively large neighborhood of the optimal point. Compared with DGC (w/o mfm), the parameter in GMC converges closer to the optimal point and then remains stable. Figure 2(a) shows

the distances to the global optimal point during the optimization process. We can find that although the momentum factor masking trick can make the convergence trajectory appear more stable, it also slows down the convergence. Figure 2(b), 2(c) and 2(d) show the distances to the global optimal point when using different s for the case when $d = 20$. We can find that, compared with the local momentum methods, the global momentum method GMC converges faster and more stably.

To gain a better intuition for the advantage of global momentum over local momentum, we rethink this simple quadratic function optimization problem by combining the update rule of the momentum term in Section 2.3. In local momentum methods, $\mathbf{m}_{t,k}$ only accumulates $\nabla F_k(\mathbf{w}_t)$, which is the gradient of $F_k(\mathbf{w})$ on worker k . The gradients of $F_k(\mathbf{w})$ tend to help the parameter to converge to the optimal point of $F_k(\mathbf{w})$ instead of the optimal point of $F(\mathbf{w})$, i.e., local momentum accumulates biased gradients during the optimization process. As for global momentum, the momentum term $-(\mathbf{w}_t - \mathbf{w}_{t-1})/\eta$ contains global information from all the workers. Since we are optimizing the objective function $F(\mathbf{w})$, $\mathbf{w}_t - \mathbf{w}_{t-1}$ denotes the descent direction of $F(\mathbf{w})$ with high probability in the next iteration, which will help the parameter to converge to the global optimal point. If no sparse communication is adopted, DGC (w/o mfm) will degenerate to DMSGD, and DGC (w/ mfm) will degenerate to DSGD. But if we adopt sparse communication, only a few components of the vectors will be communicated. The biases of the local momentums will disrupt the convergence because of the existence of compressed errors.

We have only considered a simple quadratic function optimization problem here. When it comes to deep model training, the objective functions are typically high-dimensional, non-convex, and characterized by numerous local minima and saddle points, which are much more complex than the above example. Furthermore, when we distribute the training across multiple workers, the local objective functions may differ from each other due to the heterogeneous training data distribution. In Section 5, we will demonstrate that the global momentum method outperforms its local momentum counterparts in distributed deep model training.

3.3 Convergence of GMC

In this section, we prove the convergence of GMC for non-convex problems. Here, we only present the main Lemmas and Theorems, and the proof details can be found in Appendix B. Firstly, we make the following assumptions, which are widely used in existing communication compression methods (Basu et al., 2019; Xie et al., 2020; Koloskova et al., 2020; Xu and Huang, 2022):

Assumption 1 For the compressor $\mathcal{C} : \mathbb{R}^d \rightarrow \mathbb{R}^d$, we assume that it's a δ -approximate compressor, i.e., there exists a constant $\delta \in (0, 1]$, such that

$$\mathbb{E}_{\mathcal{C}} \|\mathcal{C}(\mathbf{w}) - \mathbf{w}\|^2 \leq (1 - \delta) \|\mathbf{w}\|^2, \forall \mathbf{w} \in \mathbb{R}^d.$$

Assumption 2 For any stochastic gradient $\nabla f(\mathbf{w}; \xi)$, where ξ is randomly sampled from local dataset \mathcal{D}_k on worker k , $\forall k \in [K]$, we assume it's unbiased and variance bounded, i.e.,

$$\mathbb{E}_{\xi \sim \mathcal{D}_k} [\nabla f(\mathbf{w}; \xi)] = \nabla F_k(\mathbf{w}), \forall \mathbf{w} \in \mathbb{R}^d, \forall k \in [K];$$

$$\mathbb{E}_{\xi \sim \mathcal{D}_k} \|\nabla f(\mathbf{w}; \xi) - \nabla F_k(\mathbf{w})\|^2 \leq \sigma^2, \forall \mathbf{w} \in \mathbb{R}^d, \forall k \in [K].$$

Furthermore, the second moment of the full gradient is also bounded, i.e.,

$$\|\nabla F_k(\mathbf{w})\|^2 \leq M^2, \forall \mathbf{w} \in \mathbb{R}^d, \forall k \in [K].$$

It implies that the stochastic gradients are bounded: $\mathbb{E}_{\xi \sim \mathcal{D}_k} \|\nabla f(\mathbf{w}; \xi)\|^2 \leq G^2 \triangleq \sigma^2 + M^2, \forall \mathbf{w} \in \mathbb{R}^d, \forall k \in [K]$.

Assumption 3 For any $k \in [K]$, $F_k(\mathbf{w})$ is L -smooth ($L > 0$):

$$F_k(\mathbf{w}) - F_k(\mathbf{w}') - \nabla F_k(\mathbf{w}')^T (\mathbf{w} - \mathbf{w}') \leq \frac{L}{2} \|\mathbf{w} - \mathbf{w}'\|^2, \forall \mathbf{w}, \mathbf{w}' \in \mathbb{R}^d, \forall k \in [K].$$

Assumption 4 The objective function $F(\mathbf{w})$ is lower bounded by F^* : $F(\mathbf{w}) \geq F^*, \forall \mathbf{w} \in \mathbb{R}^d$.

We define $\nabla f(\mathbf{w}_t; \mathcal{I}_t) = \frac{1}{K} \sum_{k \in [K]} \nabla f(\mathbf{w}_t; \mathcal{I}_{t,k})$, $\bar{\mathbf{e}}_t = \frac{1}{K} \sum_{k \in [K]} \mathbf{e}_{t,k}$. By eliminating $\mathcal{C}(\cdot)$, the update rule in Algorithm 1 can be rewritten as:

$$\mathbf{w}_{t+1} = \mathbf{w}_t - \eta \nabla f(\mathbf{w}_t; \mathcal{I}_t) - \eta \bar{\mathbf{e}}_t + \eta \bar{\mathbf{e}}_{t+1} + \beta (\mathbf{w}_t - \mathbf{w}_{t-1}). \quad (7)$$

We can find that if we do not use the sparse communication technique, then $\bar{\mathbf{e}}_t = \mathbf{0}$ and (7) is the same as MSGD in (3).

We introduce an auxiliary variable \mathbf{z}_t and have the following lemma:

Lemma 3 Let $\mathbf{z}_t \triangleq \mathbf{w}_t + \frac{\beta}{1-\beta} (\mathbf{w}_t - \mathbf{w}_{t-1}) - \frac{\eta}{1-\beta} \bar{\mathbf{e}}_t$, then we have:

$$\mathbf{z}_{t+1} = \mathbf{z}_t - \frac{\eta}{1-\beta} \nabla f(\mathbf{w}_t; \mathcal{I}_t). \quad (8)$$

Equation (8) is similar to the update equation in SGD. Inspired by this, we only need to prove the convergence of \mathbf{z}_t and bound the gap $\|\mathbf{z}_t - \mathbf{w}_t\|$.

The error residual $\mathbf{e}_{t,k}$ on each worker has the following property:

Lemma 4 With Assumption 1, 2, if $\beta \leq \frac{\delta}{4\sqrt{2+\delta}}$, the error residual can be bounded:

$$\frac{1}{K} \sum_{k \in [K]} \mathbb{E} \|\mathbf{e}_{t,k}\|^2 \leq E^2,$$

$$\text{where } E^2 = \frac{(1-\delta)(1+\frac{4}{\delta})G^2}{1 - [(1-\frac{\delta}{4})(1-\frac{\beta}{K})^2 + (1+\frac{\delta}{4})(1+\frac{2}{\delta})\beta^2]}.$$

For the auxiliary variable \mathbf{z}_t in Lemma 3, the gap between \mathbf{z}_t and \mathbf{w}_t has the following property:

Lemma 5 The gap between \mathbf{z}_t and \mathbf{w}_t can be bounded: $\mathbb{E} \|\mathbf{z}_t - \mathbf{w}_t\|^2 \leq C_1 \eta^2$, where $C_1 = \frac{6(2E^2+G^2)\beta^2}{(1-\beta)^4} + \frac{2E^2}{(1-\beta)^2}$.

Then we have the following convergence result:

Theorem 6 *With Assumptions 1, 2, 3 and 4, if $\beta \leq \frac{\delta}{4\sqrt{2+\delta}}$ and $\eta \leq \frac{1-\beta}{2L}$, Algorithm 1 has the following convergence rate:*

$$\frac{1}{T} \sum_{t \in [T]} \mathbb{E} \|\nabla F(\mathbf{w}_t)\|^2 \leq \frac{4(1-\beta)(F(\mathbf{z}_0) - F^*)}{T\eta} + \frac{2L\sigma^2}{(1-\beta)b} \frac{\eta}{K} + 2C_1 L^2 \eta^2,$$

where $C_1 = \frac{6(2E^2+G^2)\beta^2}{(1-\beta)^4} + \frac{2E^2}{(1-\beta)^2}$.

Remark 7 *By taking $\eta = \mathcal{O}(\sqrt{\frac{K}{T}})$ and assuming that T is large enough (i.e., $T = \Omega(K^3)$), we can get the convergence rate of GMC to a critical point: $\frac{1}{T} \sum_{t \in [T]} \mathbb{E} \|\nabla F(\mathbf{w}_t)\|^2 \leq \mathcal{O}(\frac{1}{\sqrt{KT}})$, which is the same as that of vanilla MSGD. It also indicates that the convergence rate of GMC has a linear speedup guarantee with respect to the number of workers K .*

Remark 8 *Note that we impose a constraint on the momentum coefficient β during the theoretical proof. But in practice, even when the constraint is relaxed, e.g., $\beta = 0.9$, GMC still converges well. More details about the convergence performance of GMC are provided in Section 5.*

4 GMC+

The most widely used sparsification compressor adopted in sparse communication methods is top- s , which selects s largest components according to their absolute values. However, the top- s compressor requires extra computation overhead to find the largest components and extra communication overhead to communicate the indices of the components. Some works (Vogels et al., 2019; Xie et al., 2020; Xu and Huang, 2022) consider Random Blockwise Gradient Sparsification (RBGS) compressor, which randomly selects a block which contains s components using the same random seed among the workers.

Due to the larger compressed error introduced by RBGS compared with top- s when selecting the same number of components of the original vector to communicate, vanilla error feedback methods usually fail to converge. Xu and Huang (2022) propose DEF-A to solve the convergence problem by using detached error feedback (DEF) technique¹. The momentum variant of DEF-A in (Xu and Huang, 2022) uses local momentum. We improve DEF-A by changing its local momentum to global momentum, getting a new method called GMC+. The detail of GMC+ is shown in Algorithm 2. We also adopt parameter server architecture for illustration. GMC+ can also be easily implemented on all-reduce frameworks.

Different from GMC, each worker in GMC+ evaluates the gradient at $\mathbf{w}_{t,k}$ rather than the current parameter \mathbf{w}_t . $\mathbf{w}_{t,k}$ is a point detached from the current parameter \mathbf{w}_t using the error residual $\mathbf{e}_{t,k}$ with a tuned hyperparameter λ . When the detached coefficient λ is set as 0, GMC+ will degenerate to GMC.

We also provide the convergence analysis for GMC+. Here, we only present the main Lemmas and Theorems, and the detailed proof can be found in Appendix C. We define

1. Xu and Huang (2022) proposes two algorithms: DEF and DEF-A. Since DEF-A enhances the generalization performance of DEF, we only consider DEF-A in this paper.

Algorithm 2 GMC+

```

1: Input: sparsification compressor  $\mathcal{C}(\cdot)$ , number of workers  $K$ , number of iterations  $T$ ,
   model parameters  $\mathbf{w}_0$ , learning rate  $\eta$ , detached coefficient  $\lambda \in [0, 1]$ , momentum coefficient
    $\beta \in [0, 1)$ , training dataset  $\mathcal{D}_k, \forall k \in [K]$ ;
2: Set  $\mathbf{w}_{-1} = \mathbf{w}_0$ ,  $\mathbf{w}_{0,k} = \mathbf{w}_0$ ,  $\mathbf{e}_{0,k} = \mathbf{0}, \forall k \in [K]$ ;
3: for iteration  $t \in [T]$  do
4:   Workers:
5:   for worker  $k \in [K]$  parallelly do
6:     Randomly pick a mini-batch of training data  $\mathcal{I}_{t,k} \subseteq \mathcal{D}_k$  with  $|\mathcal{I}_{t,k}| = b$  and compute
        $\nabla f(\mathbf{w}_{t,k}; \mathcal{I}_{t,k}) = \frac{1}{b} \sum_{\xi \in \mathcal{I}_{t,k}} \nabla f(\mathbf{w}_{t,k}; \xi)$ ;
7:      $\mathbf{e}_{t+\frac{1}{2},k} = \mathbf{e}_{t,k} + \nabla f(\mathbf{w}_{t,k}; \mathcal{I}_{t,k}) - \frac{\beta}{\eta}(\mathbf{w}_t - \mathbf{w}_{t-1})$ ;
8:     Generate a sparse vector  $\mathcal{C}(\mathbf{e}_{t+\frac{1}{2},k})$  and send  $\mathcal{C}(\mathbf{e}_{t+\frac{1}{2},k})$  to the server;
9:     Update the error residual  $\mathbf{e}_{t+1,k} = \mathbf{e}_{t+\frac{1}{2},k} - \mathcal{C}(\mathbf{e}_{t+\frac{1}{2},k})$ ;
10:    Receive  $\mathbf{w}_{t+1} - \mathbf{w}_t$  from server;
11:    Get  $\mathbf{w}_{t+1}$  by  $\mathbf{w}_{t+1} = \mathbf{w}_t + (\mathbf{w}_{t+1} - \mathbf{w}_t)$ ;
12:     $\mathbf{w}_{t+1,k} = \mathbf{w}_{t+1} - \lambda\eta\mathbf{e}_{t+1,k}$  //detach
13:  end for
14:  Server:
15:  Receive  $\mathcal{C}(\mathbf{e}_{t+\frac{1}{2},k})$  from all the workers;
16:   $\mathbf{w}_{t+1} = \mathbf{w}_t - \eta\frac{1}{K} \sum_{k \in [K]} \mathcal{C}(\mathbf{e}_{t+\frac{1}{2},k})$ ;
17:  Send  $\mathbf{w}_{t+1} - \mathbf{w}_t$  to workers;
18: end for
    
```

$\bar{\mathbf{w}}_t = \frac{1}{K} \sum_{k \in [K]} \mathbf{w}_{t,k}$, $\bar{\mathbf{e}}_t = \frac{1}{K} \sum_{k \in [K]} \mathbf{e}_{t,k}$. The update rule of $\bar{\mathbf{w}}_t$ in Algorithm 2 can be rewritten as

$$\bar{\mathbf{w}}_{t+1} = \bar{\mathbf{w}}_t + \beta(\bar{\mathbf{w}}_t - \bar{\mathbf{w}}_{t-1}) + \eta(1 - \lambda)(\bar{\mathbf{e}}_{t+1} - \bar{\mathbf{e}}_t) + \beta\lambda\eta(\bar{\mathbf{e}}_t - \bar{\mathbf{e}}_{t-1}) - \eta\frac{1}{K} \sum_{k \in [K]} \nabla f(\mathbf{w}_{t,k}; \mathcal{I}_{t,k}).$$

The error residual $\mathbf{e}_{t,k}$ in Algorithm 2 has the same property as that in Algorithm 1:

Lemma 9 *With Assumption 1, 2, if $\beta \leq \frac{\delta}{4\sqrt{2+\delta}}$, the error residual can be bounded:*

$$\frac{1}{K} \sum_{k \in [K]} \mathbb{E} \|\mathbf{e}_{t,k}\|^2 \leq E^2,$$

where $E^2 = \frac{(1-\delta)(1+\frac{4}{\delta})G^2}{1 - [(1-\frac{\delta}{4})(1-\frac{\beta}{K})^2 + (1+\frac{\delta}{4})(1+\frac{\beta}{K})^2\beta^2]}$.

Lemma 10 *Let $\bar{\mathbf{z}}_t \triangleq \bar{\mathbf{w}}_t + \frac{\beta}{1-\beta}(\bar{\mathbf{w}}_t - \bar{\mathbf{w}}_{t-1}) - \frac{1}{1-\beta}[(1-\lambda)\eta\bar{\mathbf{e}}_t + \beta\lambda\eta\bar{\mathbf{e}}_{t-1}]$, then we have:*

$$\bar{\mathbf{z}}_{t+1} = \bar{\mathbf{z}}_t - \frac{\eta}{1-\beta} \frac{1}{K} \sum_{k \in [K]} \nabla f(\mathbf{w}_{t,k}; \mathcal{I}_{t,k}).$$

Lemma 11 *The gap between $\bar{\mathbf{z}}_t$ and $\bar{\mathbf{w}}_t$ can be bounded: $\mathbb{E} \|\bar{\mathbf{z}}_t - \bar{\mathbf{w}}_t\|^2 \leq C_2\eta^2$, where $C_2 = \frac{20\beta^2((1-\lambda)^2 + \beta^2\lambda^2)E^2 + 10\beta^2G^2}{(1-\beta)^4} + \frac{4E^2((1-\lambda)^2 + \beta^2\lambda^2)}{(1-\beta)^2}$.*

Theorem 12 *With Assumptions 1, 2, 3 and 4, if $\beta \leq \frac{\delta}{4\sqrt{2+\delta}}$ and $\eta \leq \frac{3(1-\beta)}{4L}$, Algorithm 2 has the following convergence rate:*

$$\frac{1}{T} \sum_{t \in [T]} \mathbb{E} \|\nabla F(\mathbf{w}_t)\|^2 \leq \frac{2(1-\beta)(F(\bar{\mathbf{z}}_0) - F^*)}{T\eta} + \frac{L\sigma^2}{(1-\beta)b} \frac{\eta}{K} + (8C_2 + 10\lambda^2 E^2)L^2\eta^2,$$

$$\text{where } C_2 = \frac{20\beta^2((1-\lambda)^2 + \beta^2\lambda^2)E^2 + 10\beta^2 G^2}{(1-\beta)^4} + \frac{4E^2((1-\lambda)^2 + \beta^2\lambda^2)}{(1-\beta)^2}.$$

Remark 13 *By taking $\eta = \mathcal{O}(\sqrt{\frac{K}{T}})$ and assuming that T is large enough (i.e., $T = \Omega(K^3)$), we can get the convergence rate of GMC+ to a critical point: $\frac{1}{T} \sum_{t \in [T]} \mathbb{E} \|\nabla F(\mathbf{w}_t)\|^2 \leq \mathcal{O}(\frac{1}{\sqrt{KT}})$, which is the same as that of GMC.*

Remark 14 *Note that the convergence guarantee of DEF-A and its momentum variant for non-convex problems is lacking in (Xu and Huang, 2022). We provide the convergence analysis for GMC+, which can be seen as a global momentum variant of DEF-A. We eliminate the assumption of ring-allreduce compatibility from (Xu and Huang, 2022) and only assume that the compressor has the δ -approximate property. This makes our convergence analysis for GMC+ applicable to a broader range of compressors, such as top-s, which is not ring-allreduce compatible.*

5 Experiments

In this section, we evaluate the performance of GMC and other baselines in image classification tasks. The experiments are conducted on a distributed platform with dockers. Each docker has access to one V100 GPU. All the experiments are implemented based on the parameter server framework.

Since the server is typically the busiest node in parameter server architecture, we consider the communication cost on the server in our experiments. For DMSGD which doesn't use any communication compression techniques, the communication cost on the server includes receiving vectors from the K workers and sending one vector to the K workers for every iteration. So the communication cost of DMSGD is $2dKT$, where d is the dimension of the model parameter, T is the number of iterations and K is the number of workers. In sparse communication methods, since only a few components of the original vector will be communicated, workers typically communicate the sparsified vectors with the server by using the structure of $(index, value)$ to denote each component. The communication cost for communicating each $(index, value)$ will be twice that for only communicating $value$ in DMSGD. For a sparse communication algorithm, we define the *relative communication cost* (RCC) as the ratio of its communication cost on the server to that of the DMSGD algorithm. We take GMC as an example to further illustrate how RCC is calculated. In GMC, the communication cost of receiving sparsified vectors from workers is $2 \sum_{t \in [T]} \sum_{k \in [K]} \|\mathcal{C}(\mathbf{e}_{t+\frac{1}{2},k})\|_0$ and the communication cost of sending aggregated sparsified vectors to workers is $2K \sum_{t \in [T]} \|\mathbf{w}_{t+1} - \mathbf{w}_t\|_0$. Hence, the total communication cost of GMC during the whole training process is $2(\sum_{t \in [T]} (\sum_{k \in [K]} \|\mathcal{C}(\mathbf{e}_{t+\frac{1}{2},k})\|_0 + K\|\mathbf{w}_{t+1} - \mathbf{w}_t\|_0))$. The

RCC of GMC is:

$$\text{RCC} = \frac{1}{dKT} \sum_{t \in [T]} (K \|\mathbf{w}_{t+1} - \mathbf{w}_t\|_0 + \sum_{k \in [K]} \|\mathcal{C}(\mathbf{e}_{t+\frac{1}{2},k})\|_0). \quad (9)$$

The RCC of DMSGD is 100% (no compression). Here, all numbers have the same unit (float value).

We use the CIFAR10 and CIFAR100 datasets under both IID and non-IID data distribution. For the IID scenario, the training data is randomly assigned to each worker. For the non-IID scenario, we use Dirichlet distribution with parameter 0.1 to partition the training data as in (Hsu et al., 2019; Lin et al., 2021). We adopt two popular deep models: ResNet20 (He et al., 2016) and Vision Transformer (ViT) (Lee et al., 2021) with four Transformer blocks. Although Batch Normalization (BN) in ResNet20 is effective in practice, it is known to be problematic in the non-IID setting due to its dependence on the estimated mean and variance (Hsieh et al., 2020). We replace BN in ResNet20 with Group Normalization (GN) (Wu and He, 2018) under non-IID data distribution as suggested in (Hsieh et al., 2020; Lin et al., 2021). We train the models with 200 epochs.

5.1 Results of GMC

We compare GMC with DGC (w/ and w/o mfm) (Lin et al., 2018), CSER (Xie et al., 2020) and DEF-A (Xu and Huang, 2022). In the experiments of (Lin et al., 2018), DGC gets far better performance on both accuracy and communication cost than quantization methods. Hence, we do not compare with quantization methods in this paper. We don't use the warm-up strategy in the experiments. The momentum coefficient β is set as 0.9. The weight decay is set as 0.0001. We use 8 workers with a total batch size of 128. We adopt the cosine annealing learning rate decay strategy (Loshchilov and Hutter, 2017) (without restarts). In the m -th epoch, the learning rate is $\eta_m = \eta * 0.5 * (1 + \cos(m\pi/200))$. For all the sparse communication algorithms, the top- s compressor is adopted to sparsify the vectors. In DGC, DEF-A and GMC, we set $s = \frac{d}{1024}$. In CSER, there are two compressors $\mathcal{C}_1, \mathcal{C}_2$ and one synchronization interval H that determine RCC together. Following the hyperparameter settings in (Xie et al., 2020), we set $s = \frac{d}{32}$ for \mathcal{C}_1 , $s = \frac{d}{2048}$ for \mathcal{C}_2 and $H = 64$. In DEF-A, the hyperparameter λ is set as 0.3 as suggested in (Xu and Huang, 2022). Considering the computation overhead of the top- s selection, we use an approximate way to implement it (Lin et al., 2018): given a vector $\mathbf{a} \in \mathbb{R}^d$, we first randomly choose a subset $S \subset [d]$ such that $|S| = \frac{d}{100}$. We get the threshold θ such that $|\{j | |a^{(j)}| \geq \theta, j \in S\}| = \frac{|S|}{1024}$. Then we set $\mathcal{C}(\mathbf{a})$ by choosing the indices in $\{j | |a^{(j)}| \geq \theta, j \in [d]\}$. It implies that $\|\mathcal{C}(\mathbf{a})\|_0$ is approximately $\frac{d}{1024}$.

Table 1 shows the empirical results of different methods under IID data distribution. Figure 3 shows the training curves under IID data distribution. We can observe that each method achieves comparable RCC. As for test accuracy, GMC and DGC (w/ mfm) exhibit comparable performance and outperform the other three methods. Table 2 and Figure 4 show the performance under non-IID data distribution. We can find that GMC can achieve much better test accuracy and faster convergence speed compared to other methods. Furthermore, we can find that the momentum factor masking trick will severely impair the performance of DGC under non-IID data distribution.

Table 1: Empirical results of different methods under IID data distribution.

Dataset	Model	Method	DGC (w/ mfm)	DGC (w/o mfm)	CSER	DEF-A	GMC
CIFAR10	ResNet20 (BN)	Accuracy	92.44%	92.30%	91.70%	92.29%	92.30%
		RCC	0.66%	0.66%	0.62%	0.65%	0.64%
	ViT	Accuracy	83.67%	83.35%	76.81%	82.67%	83.46%
		RCC	0.82%	0.81%	0.62%	0.81%	0.80%
CIFAR100	ResNet20 (BN)	Accuracy	68.05%	68.66%	66.62%	68.72%	68.89%
		RCC	0.64%	0.64%	0.65%	0.64%	0.64%
	ViT	Accuracy	59.28%	59.15%	50.35%	56.56%	59.28%
		RCC	0.80%	0.79%	0.65%	0.79%	0.78%

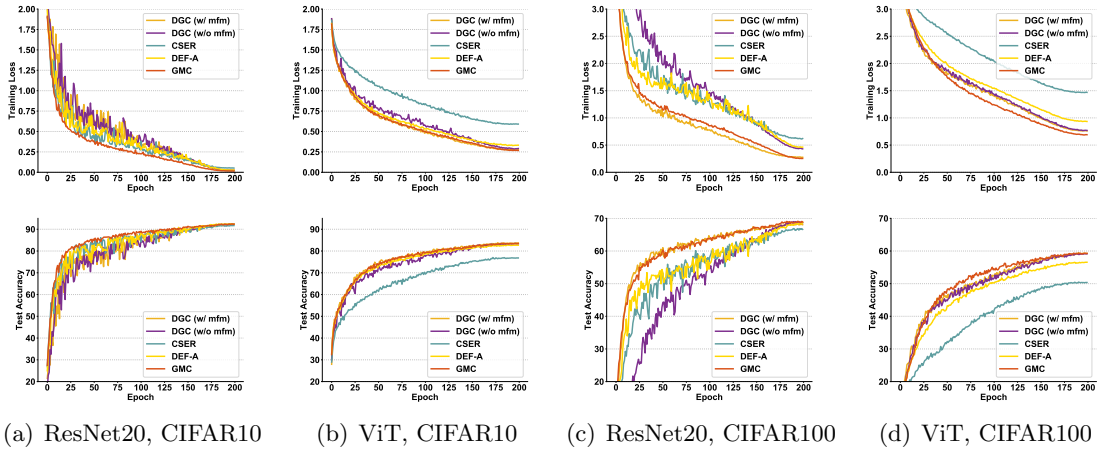


Figure 3: Training curves of different methods under IID data distribution.

Table 2: Empirical results of different methods under non-IID data distribution.

Dataset	Model	Method	DGC (w/ mfm)	DGC (w/o mfm)	CSER	DEF-A	GMC
CIFAR10	ResNet20 (GN)	Accuracy	67.13%	81.93%	78.65%	82.15%	86.51%
		RCC	0.65%	0.65%	0.63%	0.65%	0.64%
	ViT	Accuracy	60.24%	71.35%	67.35%	72.25%	73.34%
		RCC	0.81%	0.81%	0.67%	0.81%	0.81%
CIFAR100	ResNet20 (GN)	Accuracy	50.02%	52.79%	50.17%	52.07%	58.59%
		RCC	0.64%	0.64%	0.65%	0.64%	0.63%
	ViT	Accuracy	53.29%	55.00%	45.91%	50.74%	57.77%
		RCC	0.79%	0.80%	0.70%	0.79%	0.79%

5.2 Results of GMC+

To further verify the superiority of global momentum, we also evaluate DEF-A and GMC+ when using the RBGS compressor. In RBGS, we randomly select a block that contains s components using the same random seed among the workers, where $\frac{s}{d} = \frac{1}{1024}$. Since the components being communicated among the workers have the same indices, there is

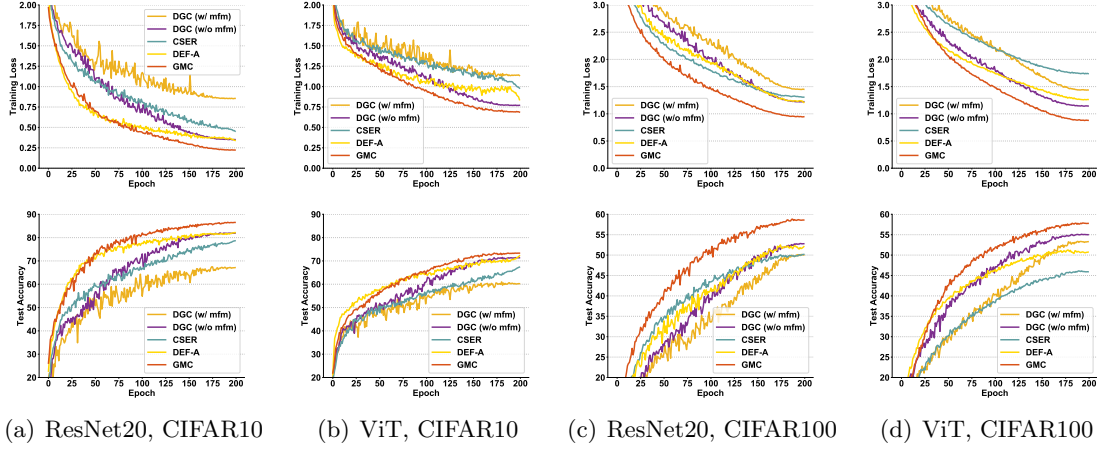


Figure 4: Training curves of different methods under non-IID data distribution.

 Table 3: Empirical results with various settings of λ in ResNet20/CIFAR100 training under IID data distribution.

	λ	0.0	0.3	0.5	0.8	1.0
DEF-A	Training Loss	4.09	0.56	0.57	0.68	0.76
	Test Accuracy	6.03%	66.36%	65.28%	64.84%	64.45%
GMC+	Training Loss	3.48	0.55	0.40	0.42	0.43
	Test Accuracy	15.81%	67.31%	67.94%	67.27%	66.68%

no need to send the indices during communication. Hence, the communication cost of receiving sparsified vectors from the workers for RBGS will be half of that for top- s : $\sum_{t \in [T]} (\sum_{k \in [K]} \|\mathcal{C}(\mathbf{e}_{t+\frac{1}{2},k})\|_0)$, where $\|\mathcal{C}(\mathbf{e}_{t+\frac{1}{2},k})\|_0/d = \frac{1}{1024}$. Similarly, the communication cost of sending aggregated sparsified vectors to workers will be $K \sum_{t \in [T]} \|\mathbf{w}_{t+1} - \mathbf{w}_t\|_0$. Since the sparsified vectors $\mathcal{C}(\mathbf{e}_{t+\frac{1}{2},k})$ have the same indices across all the workers, the aggregated sparsified vector satisfies $\|\mathbf{w}_{t+1} - \mathbf{w}_t\|_0/d = \frac{1}{1024}$. The RCC of both DEF-A and GMC+ with the above settings for the compressor can be directly calculated as follows:

$$\text{RCC} = \frac{1}{2dKT} \sum_{t \in [T]} (K \|\mathbf{w}_{t+1} - \mathbf{w}_t\|_0 + \sum_{k \in [K]} \|\mathcal{C}(\mathbf{e}_{t+\frac{1}{2},k})\|_0) = \frac{1}{1024} \approx 0.098\%.$$

The empirical results of DEF-A and GMC+ with various settings of λ in ResNet20/CIFAR100 training are shown in Table 3. Both DEF-A and GMC+ almost fail to converge when $\lambda = 0$. DEF-A achieves its best performance when $\lambda = 0.3$. In comparison, GMC+ outperforms DEF-A across different λ values and shows a preference for a larger λ (e.g., 0.5). In the following experiments, we set λ as 0.3 for DEF-A and 0.5 for GMC+. $\lambda = 0.3$ is also recommended for DEF-A in (Xu and Huang, 2022).

Table 4, Figure 5 and Figure 6 show the performance of DEF-A and GMC+. Compared with DEF-A, the global momentum method GMC+ demonstrates better test accuracy and stable convergence behavior for both IID and non-IID cases.

Table 4: Test accuracy of DEF-A and GMC+.

Dataset	Data Distribution	Model	DEF-A	GMC+
CIFAR10	IID	ResNet20 (BN)	90.78%	91.41%
		ViT	74.21%	75.78%
	non-IID	ResNet20 (GN)	78.17%	79.25%
		ViT	65.16%	66.61%
CIFAR100	IID	ResNet20 (BN)	66.36%	67.94%
		ViT	50.85%	55.50%
	non-IID	ResNet20 (GN)	49.39%	51.22%
		ViT	46.09%	50.07%

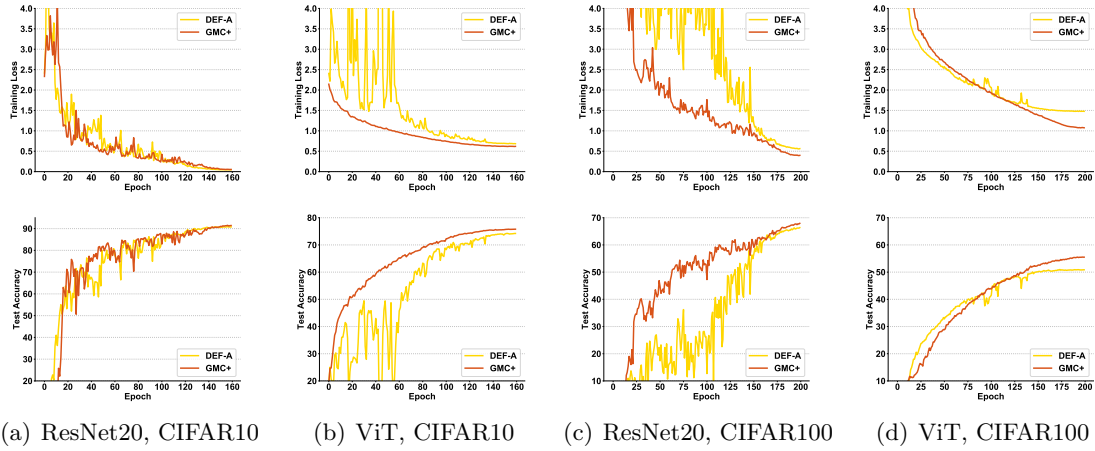


Figure 5: Training curves of DEF-A and GMC+ under IID data distribution.

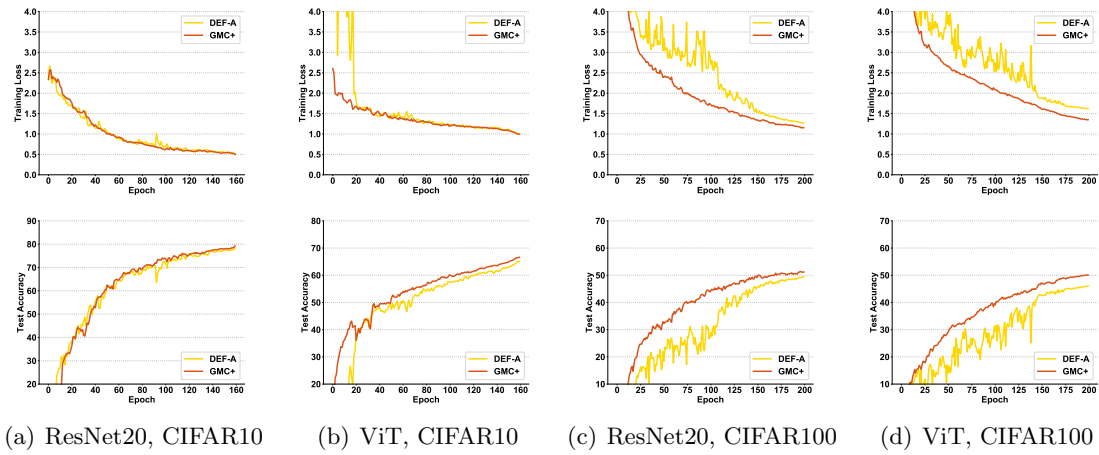


Figure 6: Training curves of DEF-A and GMC+ under non-IID data distribution.

6 Conclusion

In this paper, we propose a novel method, called *global momentum compression* (GMC), for sparse communication in distributed learning. To the best of our knowledge, this is the first work that introduces global momentum for sparse communication in DMSGD. Furthermore, to enhance the convergence performance when using more aggressive sparsification compressors (e.g., RBGS), we extend GMC to GMC+. We prove the convergence of GMC and GMC+ theoretically. Empirical results verify the superiority of global momentum and show that GMC and GMC+ can outperform other baselines to achieve state-of-the-art performance.

Appendix A. Other Ways for Combining Momentum and Error Feedback

It is easy to get one way to combine error feedback and momentum by which we can put the momentum term $\mathbf{w}_t - \mathbf{w}_{t-1}$ on the server. After receiving sparsified vectors from workers, the server updates the parameter using the momentum. We briefly present it in Algorithm 3.

Algorithm 3 Error Feedback with Momentum (momentum on server)

for iteration $t \in [T]$ **do**

Workers:

for worker $k \in [K]$ **parallelly do**

 Randomly pick a mini-batch of training data $\mathcal{I}_{t,k} \subseteq \mathcal{D}_k$ with $|\mathcal{I}_{t,k}| = b$ and compute $\nabla f(\mathbf{w}_t; \mathcal{I}_{t,k}) = \frac{1}{b} \sum_{\xi \in \mathcal{I}_{t,k}} \nabla f(\mathbf{w}_t; \xi)$;

$\mathbf{e}_{t+\frac{1}{2},k} = \mathbf{e}_{t,k} + \nabla f(\mathbf{w}_t; \mathcal{I}_{t,k})$;

 Generate a sparse vector $\mathcal{C}(\mathbf{e}_{t+\frac{1}{2},k})$ and send $\mathcal{C}(\mathbf{e}_{t+\frac{1}{2},k})$ to the server;

 Update the error residual $\mathbf{e}_{t+1,k} = \mathbf{e}_{t+\frac{1}{2},k} - \mathcal{C}(\mathbf{e}_{t+\frac{1}{2},k})$;

 Receive $\mathbf{w}_{t+1} - \mathbf{w}_t$ from server;

 Get \mathbf{w}_{t+1} by $\mathbf{w}_{t+1} = \mathbf{w}_t + (\mathbf{w}_{t+1} - \mathbf{w}_t)$;

end for

Server:

 Receive $\mathcal{C}(\mathbf{e}_{t+\frac{1}{2},k}), k \in [K]$ from all the workers;

$\mathbf{w}_{t+1} = \mathbf{w}_t - \eta \frac{1}{K} \sum_{k \in [K]} \mathcal{C}(\mathbf{e}_{t+\frac{1}{2},k}) + \beta(\mathbf{w}_t - \mathbf{w}_{t-1})$;

 Send $\mathbf{w}_{t+1} - \mathbf{w}_t$ to workers;

end for

Let $\{\mathbf{w}_t\}, \{\mathbf{e}_{t,k}\}$ be the sequences produced by Algorithm 3, then we can get that

$$\begin{aligned} \mathbf{w}_{t+1} &= \mathbf{w}_t - \eta \frac{1}{K} \sum_{k \in [K]} \mathcal{C}(\mathbf{e}_{t,k} + \nabla f(\mathbf{w}_t; \mathcal{I}_{t,k})) + \beta(\mathbf{w}_t - \mathbf{w}_{t-1}), \\ \mathbf{e}_{t+1,k} &= \mathbf{e}_{t,k} + \nabla f(\mathbf{w}_t; \mathcal{I}_{t,k}) - \mathcal{C}(\mathbf{e}_{t,k} + \nabla f(\mathbf{w}_t; \mathcal{I}_{t,k})), \forall k \in [K]. \end{aligned}$$

By eliminating $\mathcal{C}(\cdot)$, we obtain the same equation as that in (7). Hence, our convergence analysis is also suitable for Algorithm 3. The difference from GMC is that the error residual $\mathbf{e}_{t,k}$ in Algorithm 3 only keeps the compressed error from the stochastic gradients $\nabla f(\mathbf{w}_t; \mathcal{I}_{t,k})$. Compared with GMC, the disadvantage is that its error residual does not

contain the momentum information which can play the role of correcting the update direction. Hence, GMC gets better performance than Algorithm 3. Lin et al. (2018) also points out that Algorithm 3 has some loss of performance.

Another way is to put the learning rate η inside the error residual. We briefly present it in Algorithm 4. If the learning rate η is constant during the whole training process,

Algorithm 4 Error Feedback with Momentum (lr inside error residual)

```

for iteration  $t \in [T]$  do
  Workers:
  for worker  $k \in [K]$  parallelly do
    Randomly pick a mini-batch of training data  $\mathcal{I}_{t,k} \subseteq \mathcal{D}_k$  with  $|\mathcal{I}_{t,k}| = b$  and compute
     $\nabla f(\mathbf{w}_t; \mathcal{I}_{t,k}) = \frac{1}{b} \sum_{\xi \in \mathcal{I}_{t,k}} \nabla f(\mathbf{w}_t; \xi)$ ;
     $\mathbf{e}_{t+\frac{1}{2},k} = \mathbf{e}_{t,k} + \eta \nabla f(\mathbf{w}_t; \mathcal{I}_{t,k}) - \beta(\mathbf{w}_t - \mathbf{w}_{t-1})$ ;
    Generate a sparse vector  $\mathcal{C}(\mathbf{e}_{t+\frac{1}{2},k})$  and send  $\mathcal{C}(\mathbf{e}_{t+\frac{1}{2},k})$  to the server;
    Update the error residual  $\mathbf{e}_{t+1,k} = \mathbf{e}_{t+\frac{1}{2},k} - \mathcal{C}(\mathbf{e}_{t+\frac{1}{2},k})$ ;
    Receive  $\mathbf{w}_{t+1} - \mathbf{w}_t$  from server;
    Get  $\mathbf{w}_{t+1}$  by  $\mathbf{w}_{t+1} = \mathbf{w}_t + (\mathbf{w}_{t+1} - \mathbf{w}_t)$ ;
  end for
  Server:
   $\mathbf{w}_{t+1} = \mathbf{w}_t - \frac{1}{K} \sum_{k \in [K]} \mathcal{C}(\mathbf{e}_{t+\frac{1}{2},k})$ ;
  Send  $\mathbf{w}_{t+1} - \mathbf{w}_t$  to workers;
end for

```

Algorithm 4 is equivalent to Algorithm 1. However, we often use the learning rate decay strategy for deep model training in practice. We use η_t to denote the learning rate in iteration t . The update rule in Algorithm 4 can be rewritten as:

$$\mathbf{w}_{t+1} = \mathbf{w}_t - \frac{1}{K} \sum_{k \in [K]} \mathcal{C}(\mathbf{e}_{t,k} + \eta_t \nabla f(\mathbf{w}_t; \mathcal{I}_{t,k}) - \beta(\mathbf{w}_t - \mathbf{w}_{t-1})),$$

where

$$\mathbf{e}_{t,k} = \mathbf{e}_{t-\frac{1}{2},k} - \mathcal{C}(\mathbf{e}_{t-\frac{1}{2},k}), \mathbf{e}_{t-\frac{1}{2},k} = \mathbf{e}_{t-1,k} + \eta_{t-1} \nabla f(\mathbf{w}_{t-1}; \mathcal{I}_{t-1,k}) - \beta(\mathbf{w}_{t-1} - \mathbf{w}_{t-2}).$$

The update rule in GMC can be rewritten as:

$$\mathbf{w}_{t+1} = \mathbf{w}_t - \frac{1}{K} \sum_{k \in [K]} \mathcal{C}(\eta_t \mathbf{e}_{t,k}^{GMC} + \eta_t \nabla f(\mathbf{w}_t; \mathcal{I}_{t,k}) - \beta(\mathbf{w}_t - \mathbf{w}_{t-1})),$$

where

$$\begin{aligned} \eta_t \mathbf{e}_{t,k}^{GMC} &= \eta_t \mathbf{e}_{t-\frac{1}{2},k}^{GMC} - \mathcal{C}(\eta_t \mathbf{e}_{t-\frac{1}{2},k}^{GMC}), \\ \eta_t \mathbf{e}_{t-\frac{1}{2},k}^{GMC} &= \frac{\eta_t}{\eta_{t-1}} [\eta_{t-1} \mathbf{e}_{t-1,k}^{GMC} + \eta_{t-1} \nabla f(\mathbf{w}_{t-1}; \mathcal{I}_{t-1,k}) - \beta(\mathbf{w}_{t-1} - \mathbf{w}_{t-2})]. \end{aligned}$$

We compare $\eta_t \mathbf{e}_{t,k}^{GMC}$ in GMC and $\mathbf{e}_{t,k}$ in Algorithm 4. Since $\{\eta_t\}$ is non-increasing, $\frac{\eta_t}{\eta_{t-1}} \leq 1$. Compared with GMC, the error residual in Algorithm 4 participates in parameter

updates with a larger coefficient, which will deteriorate the convergence. Figure 7 shows the learning process of ResNet20 on CIFAR10. GMC is better than Algorithm 3 and Algorithm 4, especially under non-IID data distribution.

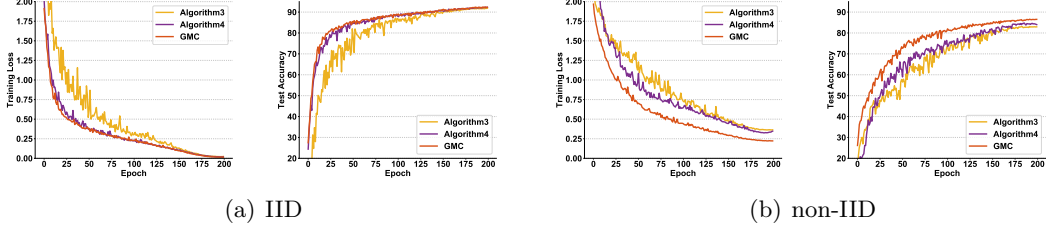


Figure 7: Comparing GMC with Algorithm 3 and Algorithm 4

Appendix B. Convergence Analysis of GMC

B.1 Proof of Lemma 3

$$\begin{aligned}
 \mathbf{z}_{t+1} &= \mathbf{w}_{t+1} + \frac{\beta}{1-\beta}(\mathbf{w}_{t+1} - \mathbf{w}_t) - \frac{\eta}{1-\beta}\bar{\mathbf{e}}_{t+1} \\
 &= \frac{1}{1-\beta}(\mathbf{w}_{t+1} - \beta\mathbf{w}_t) - \frac{\eta}{1-\beta}\bar{\mathbf{e}}_{t+1} \\
 &= \frac{1}{1-\beta}(\mathbf{w}_t - \eta\nabla f(\mathbf{w}_t; \mathcal{I}_t) + \beta(\mathbf{w}_t - \mathbf{w}_{t-1}) - \eta\bar{\mathbf{e}}_t + \eta\bar{\mathbf{e}}_{t+1} - \beta\mathbf{w}_t) - \frac{\eta}{1-\beta}\bar{\mathbf{e}}_{t+1} \\
 &= \frac{1}{1-\beta}(\mathbf{w}_t - \beta\mathbf{w}_{t-1} - \eta\nabla f(\mathbf{w}_t; \mathcal{I}_t) - \eta\bar{\mathbf{e}}_t) \\
 &= \frac{1}{1-\beta}(\mathbf{w}_t - \beta\mathbf{w}_{t-1}) - \frac{\eta}{1-\beta}\bar{\mathbf{e}}_t - \frac{\eta}{1-\beta}\nabla f(\mathbf{w}_t; \mathcal{I}_t) \\
 &= \mathbf{z}_t - \frac{\eta}{1-\beta}\nabla f(\mathbf{w}_t; \mathcal{I}_t).
 \end{aligned}$$

B.2 Proof of Lemma 4

$$\begin{aligned}
 \mathbf{e}_{t+\frac{1}{2},k} &= \mathbf{e}_{t,k} + \nabla f(\mathbf{w}_t; \mathcal{I}_{t,k}) - \frac{\beta}{\eta}(\mathbf{w}_t - \mathbf{w}_{t-1}) \\
 &= \mathbf{e}_{t,k} + \nabla f(\mathbf{w}_t; \mathcal{I}_{t,k}) + \frac{\beta}{K} \sum_{k' \in [K]} \mathcal{C}(\mathbf{e}_{t-\frac{1}{2},k'}) \\
 &= \mathbf{e}_{t-\frac{1}{2},k} - \mathcal{C}(\mathbf{e}_{t-\frac{1}{2},k}) + \frac{\beta}{K}\mathcal{C}(\mathbf{e}_{t-\frac{1}{2},k}) + \nabla f(\mathbf{w}_t; \mathcal{I}_{t,k}) + \frac{\beta}{K} \sum_{k' \in [K], k' \neq k} \mathcal{C}(\mathbf{e}_{t-\frac{1}{2},k'}) \\
 &= \mathbf{e}_{t-\frac{1}{2},k} - (1 - \frac{\beta}{K})\mathcal{C}(\mathbf{e}_{t-\frac{1}{2},k}) + \nabla f(\mathbf{w}_t; \mathcal{I}_{t,k}) + \frac{\beta}{K} \sum_{k' \in [K], k' \neq k} \mathcal{C}(\mathbf{e}_{t-\frac{1}{2},k'}) \\
 &= (1 - \frac{\beta}{K})[\mathbf{e}_{t-\frac{1}{2},k} - \mathcal{C}(\mathbf{e}_{t-\frac{1}{2},k})] + \nabla f(\mathbf{w}_t; \mathcal{I}_{t,k}) + \frac{\beta}{K}\mathbf{e}_{t-\frac{1}{2},k} + \frac{\beta}{K} \sum_{k' \in [K], k' \neq k} \mathcal{C}(\mathbf{e}_{t-\frac{1}{2},k'}).
 \end{aligned}$$

Since a sparsification compressor only selects a few components of the original vector, it's easy to verify that $\mathbb{E}_{\mathcal{C}} \|\mathcal{C}(\mathbf{w})\|^2 \leq \|\mathbf{w}\|^2, \forall \mathbf{w} \in \mathbb{R}^d$.

$$\begin{aligned}
& \mathbb{E} \|\mathbf{e}_{t+\frac{1}{2},k}\|^2 \\
&= \mathbb{E} \left\| \left(1 - \frac{\beta}{K}\right) [\mathbf{e}_{t-\frac{1}{2},k} - \mathcal{C}(\mathbf{e}_{t-\frac{1}{2},k})] + \nabla f(\mathbf{w}_t; \mathcal{I}_{t,k}) + \frac{\beta}{K} \mathbf{e}_{t-\frac{1}{2},k} + \frac{\beta}{K} \sum_{k' \in [K], k' \neq k} \mathcal{C}(\mathbf{e}_{t-\frac{1}{2},k'}) \right\|^2 \\
&\leq (1+a) \mathbb{E} \left\| \left(1 - \frac{\beta}{K}\right) [\mathbf{e}_{t-\frac{1}{2},k} - \mathcal{C}(\mathbf{e}_{t-\frac{1}{2},k})] + \frac{\beta}{K} \mathbf{e}_{t-\frac{1}{2},k} + \frac{\beta}{K} \sum_{k' \in [K], k' \neq k} \mathcal{C}(\mathbf{e}_{t-\frac{1}{2},k'}) \right\|^2 \\
&\quad + (1 + \frac{1}{a}) \mathbb{E} \|\nabla f(\mathbf{w}_t; \mathcal{I}_{t,k})\|^2 \\
&\leq (1+a)(1+b) \left(1 - \frac{\beta}{K}\right)^2 \mathbb{E} \|\mathbf{e}_{t-\frac{1}{2},k} - \mathcal{C}(\mathbf{e}_{t-\frac{1}{2},k})\|^2 \\
&\quad + (1+a)(1 + \frac{1}{b}) \mathbb{E} \left\| \frac{\beta}{K} \mathbf{e}_{t-\frac{1}{2},k} + \frac{\beta}{K} \sum_{k' \in [K], k' \neq k} \mathcal{C}(\mathbf{e}_{t-\frac{1}{2},k'}) \right\|^2 + (1 + \frac{1}{a}) \mathbb{E} \|\nabla f(\mathbf{w}_t; \mathcal{I}_{t,k})\|^2 \\
&\leq (1+a)(1+b) \left(1 - \frac{\beta}{K}\right)^2 \mathbb{E} \|\mathbf{e}_{t-\frac{1}{2},k} - \mathcal{C}(\mathbf{e}_{t-\frac{1}{2},k})\|^2 + (1+a)(1 + \frac{1}{b}) \beta^2 \frac{1}{K} \mathbb{E} \|\mathbf{e}_{t-\frac{1}{2},k}\|^2 \\
&\quad + (1+a)(1 + \frac{1}{b}) \beta^2 \frac{1}{K} \sum_{k' \in [K], k' \neq k} \mathbb{E} \|\mathcal{C}(\mathbf{e}_{t-\frac{1}{2},k'})\|^2 + (1 + \frac{1}{a}) \mathbb{E} \|\nabla f(\mathbf{w}_t; \mathcal{I}_{t,k})\|^2 \\
&\leq (1+a)(1+b) \left(1 - \frac{\beta}{K}\right)^2 (1-\delta) \mathbb{E} \|\mathbf{e}_{t-\frac{1}{2},k}\|^2 + (1+a)(1 + \frac{1}{b}) \beta^2 \frac{1}{K} \sum_{k' \in [K]} \mathbb{E} \|\mathbf{e}_{t-\frac{1}{2},k'}\|^2 \\
&\quad + (1 + \frac{1}{a}) G^2.
\end{aligned}$$

Summing up the above equation from $k = 0$ to $K - 1$, we can get

$$\begin{aligned}
\frac{1}{K} \sum_{k \in [K]} \mathbb{E} \|\mathbf{e}_{t+\frac{1}{2},k}\|^2 &\leq [(1+a)(1+b) \left(1 - \frac{\beta}{K}\right)^2 (1-\delta) + (1+a)(1 + \frac{1}{b}) \beta^2] \frac{1}{K} \sum_{k \in [K]} \mathbb{E} \|\mathbf{e}_{t-\frac{1}{2},k}\|^2 \\
&\quad + (1 + \frac{1}{a}) G^2.
\end{aligned}$$

Let $a = \frac{\delta}{4}$, $b = \frac{\delta}{2}$, we get

$$\begin{aligned}
& \frac{1}{K} \sum_{k \in [K]} \mathbb{E} \|\mathbf{e}_{t+\frac{1}{2},k}\|^2 \\
&\leq [(1 + \frac{\delta}{4})(1 + \frac{\delta}{2})(1-\delta) \left(1 - \frac{\beta}{K}\right)^2 + (1 + \frac{\delta}{4})(1 + \frac{2}{\delta}) \beta^2] \frac{1}{K} \sum_{k \in [K]} \mathbb{E} \|\mathbf{e}_{t-\frac{1}{2},k}\|^2 + (1 + \frac{4}{\delta}) G^2 \\
&\leq [(1 - \frac{\delta}{4})(1 - \frac{\beta}{K})^2 + (1 + \frac{\delta}{4})(1 + \frac{2}{\delta}) \beta^2] \frac{1}{K} \sum_{k \in [K]} \mathbb{E} \|\mathbf{e}_{t-\frac{1}{2},k}\|^2 + (1 + \frac{4}{\delta}) G^2.
\end{aligned}$$

Assuming $\beta \leq \frac{\delta}{4\sqrt{2+\delta}}$, we have

$$(1 - \frac{\delta}{4})(1 - \frac{\beta}{K})^2 + (1 + \frac{\delta}{4})(1 + \frac{2}{\delta}) \beta^2 \leq (1 - \frac{\delta}{4}) + 2(1 + \frac{2}{\delta}) \beta^2 \leq 1 - \frac{\delta}{8} < 1.$$

Then we get

$$\begin{aligned}
 \frac{1}{K} \sum_{k \in [K]} \mathbb{E} \|\mathbf{e}_{t+\frac{1}{2},k}\|^2 &\leq [(1 - \frac{\delta}{4})(1 - \frac{\beta}{K})^2 + (1 + \frac{\delta}{4})(1 + \frac{2}{\delta})\beta^2] \frac{1}{K} \sum_{k \in [K]} \mathbb{E} \|\mathbf{e}_{t-\frac{1}{2},k}\|^2 + (1 + \frac{4}{\delta})G^2 \\
 &\leq \frac{(1 + \frac{4}{\delta})G^2}{1 - [(1 - \frac{\delta}{4})(1 - \frac{\beta}{K})^2 + (1 + \frac{\delta}{4})(1 + \frac{2}{\delta})\beta^2]}. \\
 \frac{1}{K} \sum_{k \in [K]} \mathbb{E} \|\mathbf{e}_{t+1,k}\|^2 &= \frac{1}{K} \sum_{k \in [K]} \mathbb{E} \|\mathbf{e}_{t+\frac{1}{2},k} - \mathcal{C}(\mathbf{e}_{t+\frac{1}{2},k})\|^2 \leq (1 - \delta) \frac{1}{K} \sum_{k \in [K]} \mathbb{E} \|\mathbf{e}_{t+\frac{1}{2},k}\|^2 \\
 &\leq \frac{(1 - \delta)(1 + \frac{4}{\delta})G^2}{1 - [(1 - \frac{\delta}{4})(1 - \frac{\beta}{K})^2 + (1 + \frac{\delta}{4})(1 + \frac{2}{\delta})\beta^2]}.
 \end{aligned}$$

B.3 Proof of Lemma 5

$$\begin{aligned}
 \mathbb{E} \|\mathbf{w}_t - \mathbf{w}_{t-1}\|^2 &= \mathbb{E} \|\beta(\mathbf{w}_{t-1} - \mathbf{w}_{t-2}) + \eta \bar{\mathbf{e}}_t - \eta \bar{\mathbf{e}}_{t-1} - \eta \nabla f(\mathbf{w}_{t-1}; \mathcal{I}_{t-1})\|^2 \\
 &\leq (1 + a)\beta^2 \mathbb{E} \|\mathbf{w}_{t-1} - \mathbf{w}_{t-2}\|^2 + (1 + \frac{1}{a})\eta^2 \mathbb{E} \|\bar{\mathbf{e}}_t - \bar{\mathbf{e}}_{t-1} - \nabla f(\mathbf{w}_{t-1}; \mathcal{I}_{t-1})\|^2 \\
 &\leq (1 + a)\beta^2 \mathbb{E} \|\mathbf{w}_{t-1} - \mathbf{w}_{t-2}\|^2 + 3(1 + \frac{1}{a})(2E^2 + G^2)\eta^2.
 \end{aligned}$$

If $\beta \in (0, 1)$, let $a = \frac{1}{\beta} - 1$, then we have

$$\mathbb{E} \|\mathbf{w}_t - \mathbf{w}_{t-1}\|^2 \leq \beta \mathbb{E} \|\mathbf{w}_{t-1} - \mathbf{w}_{t-2}\|^2 + \frac{3(2E^2 + G^2)}{1 - \beta} \eta^2 \leq \frac{3(2E^2 + G^2)}{(1 - \beta)^2} \eta^2.$$

If $\beta = 0$, it's obvious that $\mathbb{E} \|\mathbf{w}_t - \mathbf{w}_{t-1}\|^2$ can be bounded by $\frac{3(2E^2 + G^2)}{(1 - \beta)^2} \eta^2$.

$$\begin{aligned}
 &\mathbb{E} \|\mathbf{z}_t - \mathbf{w}_t\|^2 \\
 &= \mathbb{E} \left\| \frac{\beta}{1 - \beta} (\mathbf{w}_t - \mathbf{w}_{t-1}) - \frac{\eta}{1 - \beta} \bar{\mathbf{e}}_t \right\|^2 \leq 2 \frac{\beta^2}{(1 - \beta)^2} \mathbb{E} \|\mathbf{w}_t - \mathbf{w}_{t-1}\|^2 + \frac{2\eta^2}{(1 - \beta)^2} \mathbb{E} \|\bar{\mathbf{e}}_t\|^2 \\
 &\leq 2 \frac{\beta^2}{(1 - \beta)^2} \mathbb{E} \|\mathbf{w}_t - \mathbf{w}_{t-1}\|^2 + \frac{2\eta^2}{(1 - \beta)^2} E^2 \leq \left[\frac{6(2E^2 + G^2)\beta^2}{(1 - \beta)^4} + \frac{2E^2}{(1 - \beta)^2} \right] \eta^2.
 \end{aligned}$$

B.4 Proof of Theorem 6

$$\begin{aligned}
 F(\mathbf{z}_{t+1}) &\leq F(\mathbf{z}_t) - \frac{\eta}{1 - \beta} \nabla F(\mathbf{z}_t)^T \nabla f(\mathbf{w}_t; \mathcal{I}_t) + \frac{L\eta^2}{2(1 - \beta)^2} \|\nabla f(\mathbf{w}_t; \mathcal{I}_t)\|^2 \\
 \mathbb{E} F(\mathbf{z}_{t+1}) &\leq F(\mathbf{z}_t) - \frac{\eta}{1 - \beta} \nabla F(\mathbf{z}_t)^T \mathbb{E} [\nabla f(\mathbf{w}_t; \mathcal{I}_t)] + \frac{L\eta^2}{2(1 - \beta)^2} \mathbb{E} \|\nabla f(\mathbf{w}_t; \mathcal{I}_t)\|^2 \\
 &= F(\mathbf{z}_t) - \frac{\eta}{1 - \beta} \nabla F(\mathbf{z}_t)^T \nabla F(\mathbf{w}_t) + \frac{L\eta^2}{2(1 - \beta)^2} \mathbb{E} \|\nabla f(\mathbf{w}_t; \mathcal{I}_t)\|^2.
 \end{aligned}$$

$$\begin{aligned}
-\frac{\eta}{1-\beta} \nabla F(\mathbf{z}_t)^T \nabla F(\mathbf{w}_t) &= -\frac{\eta}{1-\beta} (\nabla F(\mathbf{z}_t) - \nabla F(\mathbf{w}_t))^T \nabla F(\mathbf{w}_t) - \frac{\eta}{1-\beta} \|\nabla F(\mathbf{w}_t)\|^2 \\
&\leq \frac{\eta}{2(1-\beta)} \|\nabla F(\mathbf{z}_t) - \nabla F(\mathbf{w}_t)\|^2 - \frac{\eta}{2(1-\beta)} \|\nabla F(\mathbf{w}_t)\|^2 \\
&\leq \frac{\eta L^2}{2(1-\beta)} \|\mathbf{z}_t - \mathbf{w}_t\|^2 - \frac{\eta}{2(1-\beta)} \|\nabla F(\mathbf{w}_t)\|^2 \\
&\leq \frac{C_1 L^2}{2(1-\beta)} \eta^3 - \frac{\eta}{2(1-\beta)} \|\nabla F(\mathbf{w}_t)\|^2.
\end{aligned}$$

$$\begin{aligned}
\mathbb{E} \|\nabla f(\mathbf{w}_t; \mathcal{I}_t)\|^2 &= \mathbb{E} \left\| \frac{1}{K} \sum_{k \in [K]} [\nabla f(\mathbf{w}_t; \mathcal{I}_{t,k}) - \nabla F_k(\mathbf{w}_t)] + \frac{1}{K} \sum_{k \in [K]} \nabla F_k(\mathbf{w}_t) \right\|^2 \\
&= \mathbb{E} \left\| \frac{1}{K} \sum_{k \in [K]} (\nabla f(\mathbf{w}_t; \mathcal{I}_{t,k}) - \nabla F_k(\mathbf{w}_t)) \right\|^2 + \|\nabla F(\mathbf{w}_t)\|^2 \\
&\leq \frac{\sigma^2}{Kb} + \|\nabla F(\mathbf{w}_t)\|^2.
\end{aligned}$$

$$\begin{aligned}
\mathbb{E} F(\mathbf{z}_{t+1}) &\leq F(\mathbf{z}_t) - \frac{\eta}{1-\beta} \nabla F(\mathbf{z}_t)^T \nabla F(\mathbf{w}_t) + \frac{L\eta^2}{2(1-\beta)^2} \mathbb{E} \|\nabla f(\mathbf{w}_t; \mathcal{I}_t)\|^2 \\
&\leq F(\mathbf{z}_t) + \frac{C_1 L^2}{2(1-\beta)} \eta^3 + \frac{L\sigma^2}{2(1-\beta)^2 b} \frac{\eta^2}{K} - \left(\frac{\eta}{2(1-\beta)} - \frac{L\eta^2}{2(1-\beta)^2} \right) \|\nabla F(\mathbf{w}_t)\|^2.
\end{aligned}$$

Since we assume $\eta \leq \frac{1-\beta}{2L}$, we have $-\left(\frac{\eta}{2(1-\beta)} - \frac{L\eta^2}{2(1-\beta)^2}\right) \leq -\frac{\eta}{4(1-\beta)}$.

$$\begin{aligned}
\mathbb{E} F(\mathbf{z}_{t+1}) &\leq \mathbb{E} F(\mathbf{z}_t) + \frac{C_1 L^2}{2(1-\beta)} \eta^3 + \frac{L\sigma^2}{2(1-\beta)^2 b} \frac{\eta^2}{K} - \left(\frac{\eta}{2(1-\beta)} - \frac{L\eta^2}{2(1-\beta)^2} \right) \mathbb{E} \|\nabla F(\mathbf{w}_t)\|^2 \\
&\leq \mathbb{E} F(\mathbf{z}_t) + \frac{C_1 L^2}{2(1-\beta)} \eta^3 + \frac{L\sigma^2}{2(1-\beta)^2 b} \frac{\eta^2}{K} - \frac{\eta}{4(1-\beta)} \mathbb{E} \|\nabla F(\mathbf{w}_t)\|^2.
\end{aligned}$$

$$\mathbb{E} \|\nabla F(\mathbf{w}_t)\|^2 \leq \frac{4(1-\beta)(\mathbb{E} F(\mathbf{z}_t) - \mathbb{E} F(\mathbf{z}_{t+1}))}{\eta} + \frac{2L\sigma^2}{(1-\beta)b} \frac{\eta}{K} + 2C_1 L^2 \eta^2.$$

Summing up the above equation from $t = 0$ to $T - 1$, we have

$$\frac{1}{T} \sum_{t \in [T]} \mathbb{E} \|\nabla F(\mathbf{w}_t)\|^2 \leq \frac{4(1-\beta)(F(\mathbf{z}_0) - F^*)}{T\eta} + \frac{2L\sigma^2}{(1-\beta)b} \frac{\eta}{K} + 2C_1 L^2 \eta^2.$$

Appendix C. Convergence Analysis of GMC+

C.1 Proof of Lemma 9

The derivation details are similar to that in Lemma 4.

$$\begin{aligned}
 \mathbf{e}_{t+\frac{1}{2},k} &= \mathbf{e}_{t,k} + \nabla f(\mathbf{w}_{t,k}; \mathcal{I}_{t,k}) - \frac{\beta}{\eta}(\mathbf{w}_t - \mathbf{w}_{t-1}) \\
 &= \mathbf{e}_{t-\frac{1}{2},k} - \mathcal{C}(\mathbf{e}_{t-\frac{1}{2},k}) + \nabla f(\mathbf{w}_{t,k}; \mathcal{I}_{t,k}) + \frac{\beta}{K} \sum_{k' \in [K]} \mathcal{C}(\mathbf{e}_{t-\frac{1}{2},k'}) \\
 &= (1 - \frac{\beta}{K})[\mathbf{e}_{t-\frac{1}{2},k} - \mathcal{C}(\mathbf{e}_{t-\frac{1}{2},k})] + \nabla f(\mathbf{w}_{t,k}; \mathcal{I}_{t,k}) + \frac{\beta}{K} \mathbf{e}_{t-\frac{1}{2},k} + \frac{\beta}{K} \sum_{k' \in [K], k' \neq k} \mathcal{C}(\mathbf{e}_{t-\frac{1}{2},k'}).
 \end{aligned}$$

$$\begin{aligned}
 &\mathbb{E} \|\mathbf{e}_{t+\frac{1}{2},k}\|^2 \\
 &= \mathbb{E} \|(1 - \frac{\beta}{K})[\mathbf{e}_{t-\frac{1}{2},k} - \mathcal{C}(\mathbf{e}_{t-\frac{1}{2},k})] + \nabla f(\mathbf{w}_{t,k}; \mathcal{I}_{t,k}) + \frac{\beta}{K} \mathbf{e}_{t-\frac{1}{2},k} + \frac{\beta}{K} \sum_{k' \in [K], k' \neq k} \mathcal{C}(\mathbf{e}_{t-\frac{1}{2},k'})\|^2 \\
 &\leq (1+a)(1+b)(1 - \frac{\beta}{K})^2(1-\delta) \mathbb{E} \|\mathbf{e}_{t-\frac{1}{2},k}\|^2 + (1+a)(1 + \frac{1}{b}) \frac{\beta^2}{K} \sum_{k' \in [K]} \mathbb{E} \|\mathbf{e}_{t-\frac{1}{2},k'}\|^2 + (1 + \frac{1}{a})G^2.
 \end{aligned}$$

Summing up the above equation from $k = 0$ to $K - 1$, we can get

$$\begin{aligned}
 \frac{1}{K} \sum_{k \in [K]} \mathbb{E} \|\mathbf{e}_{t+\frac{1}{2},k}\|^2 &\leq [(1+a)(1+b)(1 - \frac{\beta}{K})^2(1-\delta) + (1+a)(1 + \frac{1}{b})\beta^2] \frac{1}{K} \sum_{k \in [K]} \mathbb{E} \|\mathbf{e}_{t-\frac{1}{2},k}\|^2 \\
 &\quad + (1 + \frac{1}{a})G^2.
 \end{aligned}$$

Let $a = \frac{\delta}{4}$, $b = \frac{\delta}{2}$, we get

$$\frac{1}{K} \sum_{k \in [K]} \mathbb{E} \|\mathbf{e}_{t+\frac{1}{2},k}\|^2 \leq [(1 - \frac{\delta}{4})(1 - \frac{\beta}{K})^2 + (1 + \frac{\delta}{4})(1 + \frac{2}{\delta})\beta^2] \frac{1}{K} \sum_{k \in [K]} \mathbb{E} \|\mathbf{e}_{t-\frac{1}{2},k}\|^2 + (1 + \frac{4}{\delta})G^2.$$

Let $\beta \leq \frac{\delta}{4\sqrt{2+\delta}}$, then we have

$$(1 - \frac{\delta}{4})(1 - \frac{\beta}{K})^2 + (1 + \frac{\delta}{4})(1 + \frac{2}{\delta})\beta^2 \leq (1 - \frac{\delta}{4}) + 2(1 + \frac{2}{\delta})\beta^2 \leq 1 - \frac{\delta}{8} < 1.$$

Then we get

$$\begin{aligned}
 \frac{1}{K} \sum_{k \in [K]} \mathbb{E} \|\mathbf{e}_{t+1,k}\|^2 &= \frac{1}{K} \sum_{k \in [K]} \mathbb{E} \|\mathbf{e}_{t+\frac{1}{2},k} - \mathcal{C}(\mathbf{e}_{t+\frac{1}{2},k})\|^2 \leq (1-\delta) \frac{1}{K} \sum_{k \in [K]} \mathbb{E} \|\mathbf{e}_{t+\frac{1}{2},k}\|^2 \\
 &\leq \frac{(1-\delta)(1 + \frac{4}{\delta})G^2}{1 - [(1 - \frac{\delta}{4})(1 - \frac{\beta}{K})^2 + (1 + \frac{\delta}{4})(1 + \frac{2}{\delta})\beta^2]}.
 \end{aligned}$$

C.2 Proof of Lemma 10

$$\begin{aligned}
\bar{\mathbf{z}}_{t+1} &= \bar{\mathbf{w}}_{t+1} + \frac{\beta}{1-\beta}(\bar{\mathbf{w}}_{t+1} - \bar{\mathbf{w}}_t) - \frac{1}{1-\beta}[(1-\lambda)\eta\bar{\mathbf{e}}_{t+1} + \beta\lambda\eta\bar{\mathbf{e}}_t] \\
&= \frac{1}{1-\beta}\bar{\mathbf{w}}_{t+1} - \frac{\beta}{1-\beta}\bar{\mathbf{w}}_t - \frac{1}{1-\beta}[(1-\lambda)\eta\bar{\mathbf{e}}_{t+1} + \beta\lambda\eta\bar{\mathbf{e}}_t] \\
&= \frac{1}{1-\beta}(\bar{\mathbf{w}}_t - \beta\bar{\mathbf{w}}_{t-1}) - \frac{1}{1-\beta}[(1-\lambda)\eta\bar{\mathbf{e}}_t + \beta\lambda\eta\bar{\mathbf{e}}_{t-1}] - \frac{\eta}{1-\beta}\frac{1}{K}\sum_{k\in[K]}\nabla f(\mathbf{w}_{t,k};\mathcal{I}_{t,k}) \\
&= \bar{\mathbf{z}}_t - \frac{\eta}{1-\beta}\frac{1}{K}\sum_{k\in[K]}\nabla f(\mathbf{w}_{t,k};\mathcal{I}_{t,k}).
\end{aligned}$$

C.3 Proof of Lemma 11

$$\begin{aligned}
&\mathbb{E}\|\bar{\mathbf{w}}_{t+1} - \bar{\mathbf{w}}_t\|^2 \\
&= \mathbb{E}\|\beta(\bar{\mathbf{w}}_t - \bar{\mathbf{w}}_{t-1}) + \eta(1-\lambda)(\bar{\mathbf{e}}_{t+1} - \bar{\mathbf{e}}_t) + \beta\lambda\eta(\bar{\mathbf{e}}_t - \bar{\mathbf{e}}_{t-1}) - \frac{\eta}{K}\sum_{k\in[K]}\nabla f(\mathbf{w}_{t,k};\mathcal{I}_{t,k})\|^2 \\
&\leq (1+a)\beta^2\mathbb{E}\|\bar{\mathbf{w}}_t - \bar{\mathbf{w}}_{t-1}\|^2 \\
&\quad + (1+\frac{1}{a})\eta^2\mathbb{E}\|(1-\lambda)(\bar{\mathbf{e}}_{t+1} - \bar{\mathbf{e}}_t) + \beta\lambda(\bar{\mathbf{e}}_t - \bar{\mathbf{e}}_{t-1}) - \frac{1}{K}\sum_{k\in[K]}\nabla f(\mathbf{w}_{t,k};\mathcal{I}_{t,k})\|^2 \\
&\leq (1+a)\beta^2\mathbb{E}\|\bar{\mathbf{w}}_t - \bar{\mathbf{w}}_{t-1}\|^2 + 5(1+\frac{1}{a})\eta^2[2(1-\lambda)^2E^2 + 2\beta^2\lambda^2E^2 + G^2].
\end{aligned}$$

If $\beta \in (0, 1)$, let $a = \frac{1}{\beta} - 1$, then we have

$$\begin{aligned}
\mathbb{E}\|\bar{\mathbf{w}}_t - \bar{\mathbf{w}}_{t-1}\|^2 &\leq \beta\mathbb{E}\|\bar{\mathbf{w}}_{t-1} - \bar{\mathbf{w}}_{t-2}\|^2 + \frac{10((1-\lambda)^2 + \beta^2\lambda^2)E^2 + 5G^2}{1-\beta}\eta^2 \\
&\leq \frac{10((1-\lambda)^2 + \beta^2\lambda^2)E^2 + 5G^2}{(1-\beta)^2}\eta^2.
\end{aligned}$$

If $\beta = 0$, it's obvious that $\mathbb{E}\|\mathbf{w}_t - \mathbf{w}_{t-1}\|^2$ can be bounded by $\frac{10((1-\lambda)^2 + \beta^2\lambda^2)E^2 + 5G^2}{(1-\beta)^2}\eta^2$.

$$\begin{aligned}
\mathbb{E}\|\bar{\mathbf{z}}_t - \bar{\mathbf{w}}_t\|^2 &= \mathbb{E}\|\frac{\beta}{1-\beta}(\bar{\mathbf{w}}_t - \bar{\mathbf{w}}_{t-1}) - \frac{1}{1-\beta}[(1-\lambda)\eta\bar{\mathbf{e}}_t + \beta\lambda\eta\bar{\mathbf{e}}_{t-1}]\|^2 \\
&\leq 2\frac{\beta^2}{(1-\beta)^2}\mathbb{E}\|\bar{\mathbf{w}}_t - \bar{\mathbf{w}}_{t-1}\|^2 + \frac{2\eta^2}{(1-\beta)^2}\mathbb{E}\|(1-\lambda)\bar{\mathbf{e}}_t + \beta\lambda\bar{\mathbf{e}}_{t-1}\|^2 \\
&\leq 2\frac{\beta^2}{(1-\beta)^2}\mathbb{E}\|\bar{\mathbf{w}}_t - \bar{\mathbf{w}}_{t-1}\|^2 + \frac{4\eta^2}{(1-\beta)^2}[(1-\lambda)^2\mathbb{E}\|\bar{\mathbf{e}}_t\|^2 + \beta^2\lambda^2\mathbb{E}\|\bar{\mathbf{e}}_{t-1}\|^2] \\
&\leq 2\frac{\beta^2}{(1-\beta)^2}\mathbb{E}\|\bar{\mathbf{w}}_t - \bar{\mathbf{w}}_{t-1}\|^2 + \frac{4\eta^2E^2((1-\lambda)^2 + \beta^2\lambda^2)}{(1-\beta)^2} \\
&\leq 2\frac{\beta^2}{(1-\beta)^2}\frac{10((1-\lambda)^2 + \beta^2\lambda^2)E^2 + 5G^2}{(1-\beta)^2}\eta^2 + \frac{4\eta^2E^2((1-\lambda)^2 + \beta^2\lambda^2)}{(1-\beta)^2} \\
&\leq [\frac{20\beta^2((1-\lambda)^2 + \beta^2\lambda^2)E^2 + 10\beta^2G^2}{(1-\beta)^4} + \frac{4E^2((1-\lambda)^2 + \beta^2\lambda^2)}{(1-\beta)^2}]\eta^2.
\end{aligned}$$

C.4 Proof of Theorem 12

$$\begin{aligned}
 \mathbb{E}F(\bar{\mathbf{z}}_{t+1}) &\leq F(\bar{\mathbf{z}}_t) - \frac{\eta}{1-\beta} \nabla F(\bar{\mathbf{z}}_t)^T \left(\frac{1}{K} \sum_{k \in [K]} \nabla F_k(\mathbf{w}_{t,k}) \right) + \frac{L\eta^2}{2(1-\beta)^2} \mathbb{E} \left\| \frac{1}{K} \sum_{k \in [K]} \nabla f(\mathbf{w}_{t,k}; \mathcal{I}_{t,k}) \right\|^2 \\
 &\quad - \frac{\eta}{1-\beta} \nabla F(\bar{\mathbf{z}}_t)^T \left(\frac{1}{K} \sum_{k \in [K]} \nabla F_k(\mathbf{w}_{t,k}) \right) \\
 &= -\frac{\eta}{1-\beta} (\nabla F(\bar{\mathbf{z}}_t) - \nabla F(\mathbf{w}_t))^T \left(\frac{1}{K} \sum_{k \in [K]} \nabla F_k(\mathbf{w}_{t,k}) \right) - \frac{\eta}{1-\beta} (\nabla F(\mathbf{w}_t))^T \left(\frac{1}{K} \sum_{k \in [K]} \nabla F_k(\mathbf{w}_{t,k}) \right) \\
 &\leq -\frac{\eta}{1-\beta} [2(\nabla F(\bar{\mathbf{z}}_t) - \nabla F(\mathbf{w}_t))]^T \left[\frac{1}{2K} \sum_{k \in [K]} \nabla F_k(\mathbf{w}_{t,k}) \right] - \frac{\eta}{1-\beta} (\nabla F(\mathbf{w}_t))^T \left(\frac{1}{K} \sum_{k \in [K]} \nabla F_k(\mathbf{w}_{t,k}) \right) \\
 &\leq \frac{2\eta}{1-\beta} \|\nabla F(\bar{\mathbf{z}}_t) - \nabla F(\mathbf{w}_t)\|^2 + \frac{\eta}{8(1-\beta)} \left\| \frac{1}{K} \sum_{k \in [K]} \nabla F_k(\mathbf{w}_{t,k}) \right\|^2 \\
 &\quad - \frac{\eta}{2(1-\beta)} [\|\nabla F(\mathbf{w}_t)\|^2 + \left\| \frac{1}{K} \sum_{k \in [K]} \nabla F_k(\mathbf{w}_{t,k}) \right\|^2 - \left\| \nabla F(\mathbf{w}_t) - \frac{1}{K} \sum_{k \in [K]} \nabla F_k(\mathbf{w}_{t,k}) \right\|^2] \\
 &\leq \frac{2\eta L^2}{1-\beta} \|\bar{\mathbf{z}}_t - \mathbf{w}_t\|^2 - \frac{\eta}{2(1-\beta)} \|\nabla F(\mathbf{w}_t)\|^2 + \frac{\eta}{2(1-\beta)} \left\| \nabla F(\mathbf{w}_t) - \frac{1}{K} \sum_{k \in [K]} \nabla F_k(\mathbf{w}_{t,k}) \right\|^2 \\
 &\quad - \frac{3\eta}{8(1-\beta)} \left\| \frac{1}{K} \sum_{k \in [K]} \nabla F_k(\mathbf{w}_{t,k}) \right\|^2.
 \end{aligned}$$

$$\begin{aligned}
 \mathbb{E} \left\| \frac{1}{K} \sum_{k \in [K]} \nabla f(\mathbf{w}_{t,k}; \mathcal{I}_{t,k}) \right\|^2 &= \mathbb{E} \left\| \frac{1}{K} \sum_{k \in [K]} (\nabla f(\mathbf{w}_{t,k}; \mathcal{I}_{t,k}) - \nabla F_k(\mathbf{w}_{t,k}) + \nabla F_k(\mathbf{w}_{t,k})) \right\|^2 \\
 &= \mathbb{E} \left\| \frac{1}{K} \sum_{k \in [K]} (\nabla f(\mathbf{w}_{t,k}; \mathcal{I}_{t,k}) - \nabla F_k(\mathbf{w}_{t,k})) \right\|^2 + \left\| \frac{1}{K} \sum_{k \in [K]} \nabla F_k(\mathbf{w}_{t,k}) \right\|^2 \\
 &= \frac{1}{K^2} \sum_{k \in [K]} \mathbb{E} \|\nabla f(\mathbf{w}_{t,k}; \mathcal{I}_{t,k}) - \nabla F_k(\mathbf{w}_{t,k})\|^2 + \left\| \frac{1}{K} \sum_{k \in [K]} \nabla F_k(\mathbf{w}_{t,k}) \right\|^2 \\
 &\leq \frac{\sigma^2}{Kb} + \left\| \frac{1}{K} \sum_{k \in [K]} \nabla F_k(\mathbf{w}_{t,k}) \right\|^2.
 \end{aligned}$$

$$\begin{aligned}
 \mathbb{E}F(\bar{\mathbf{z}}_{t+1}) &\leq F(\bar{\mathbf{z}}_t) - \frac{\eta}{1-\beta} \nabla F(\bar{\mathbf{z}}_t)^T \left(\frac{1}{K} \sum_{k \in [K]} \nabla F_k(\mathbf{w}_{t,k}) \right) + \frac{L\eta^2}{2(1-\beta)^2} \mathbb{E} \left\| \frac{1}{K} \sum_{k \in [K]} \nabla f(\mathbf{w}_{t,k}; \mathcal{I}_{t,k}) \right\|^2 \\
 &\leq F(\bar{\mathbf{z}}_t) + \frac{2\eta L^2}{1-\beta} \|\bar{\mathbf{z}}_t - \mathbf{w}_t\|^2 + \left[-\frac{3\eta}{8(1-\beta)} + \frac{L\eta^2}{2(1-\beta)^2} \right] \left\| \frac{1}{K} \sum_{k \in [K]} \nabla F_k(\mathbf{w}_{t,k}) \right\|^2 \\
 &\quad - \frac{\eta}{2(1-\beta)} \|\nabla F(\mathbf{w}_t)\|^2 + \frac{\eta}{2(1-\beta)} \left\| \nabla F(\mathbf{w}_t) - \frac{1}{K} \sum_{k \in [K]} \nabla F_k(\mathbf{w}_{t,k}) \right\|^2 + \frac{L\sigma^2}{2(1-\beta)^2 b} \frac{\eta^2}{K}.
 \end{aligned}$$

Since we assume $\eta \leq \frac{3(1-\beta)}{4L}$, we can obtain that $-\frac{3\eta}{8(1-\beta)} + \frac{L\eta^2}{2(1-\beta)^2} \leq 0$.

$$\begin{aligned} \mathbb{E}F(\bar{\mathbf{z}}_{t+1}) &\leq F(\bar{\mathbf{z}}_t) + \frac{2\eta L^2}{1-\beta} \|\bar{\mathbf{z}}_t - \mathbf{w}_t\|^2 + \frac{\eta}{2(1-\beta)} \|\nabla F(\mathbf{w}_t) - \frac{1}{K} \sum_{k \in [K]} \nabla F_k(\mathbf{w}_{t,k})\|^2 \\ &\quad + \frac{L\sigma^2}{2(1-\beta)^2 b} \frac{\eta^2}{K} - \frac{\eta}{2(1-\beta)} \|\nabla F(\mathbf{w}_t)\|^2. \end{aligned}$$

$$\begin{aligned} \mathbb{E} \|\nabla F(\mathbf{w}_t) - \frac{1}{K} \sum_{k \in [K]} \nabla F_k(\mathbf{w}_{t,k})\|^2 &= \mathbb{E} \left\| \frac{1}{K} \sum_{k \in [K]} [\nabla F_k(\mathbf{w}_t) - \nabla F_k(\mathbf{w}_{t,k})] \right\|^2 \\ &\leq \frac{1}{K} \sum_{k \in [K]} \mathbb{E} \|\nabla F_k(\mathbf{w}_t) - \nabla F_k(\mathbf{w}_{t,k})\|^2 \\ &\leq \frac{L^2}{K} \sum_{k \in [K]} \mathbb{E} \|\mathbf{w}_t - \mathbf{w}_{t,k}\|^2 \leq \frac{L^2}{K} \sum_{k \in [K]} \mathbb{E} \|\lambda \eta \mathbf{e}_{t,k}\|^2 \\ &\leq \frac{L^2 \lambda^2 \eta^2}{K} \sum_{k \in [K]} \mathbb{E} \|\mathbf{e}_{t,k}\|^2 \leq L^2 \lambda^2 E^2 \eta^2. \end{aligned}$$

$$\|\bar{\mathbf{z}}_t - \mathbf{w}_t\|^2 \leq 2\|\bar{\mathbf{z}}_t - \bar{\mathbf{w}}_t\|^2 + 2\|\bar{\mathbf{w}}_t - \mathbf{w}_t\|^2 \leq 2(C_2 + \lambda^2 E^2) \eta^2.$$

$$\begin{aligned} \mathbb{E}F(\bar{\mathbf{z}}_{t+1}) &\leq \mathbb{E}F(\bar{\mathbf{z}}_t) + \frac{2\eta L^2}{1-\beta} \|\bar{\mathbf{z}}_t - \mathbf{w}_t\|^2 + \frac{\eta}{2(1-\beta)} \mathbb{E} \|\nabla F(\mathbf{w}_t) - \frac{1}{K} \sum_{k \in [K]} \nabla F_k(\mathbf{w}_{t,k})\|^2 \\ &\quad + \frac{L\sigma^2}{2b(1-\beta)^2} \frac{\eta^2}{K} - \frac{\eta}{2(1-\beta)} \mathbb{E} \|\nabla F(\mathbf{w}_t)\|^2 \\ &\leq \mathbb{E}F(\bar{\mathbf{z}}_t) + \frac{(4C_2 + 5\lambda^2 E^2)L^2 \eta^3}{1-\beta} + \frac{L\sigma^2}{2(1-\beta)^2 b} \frac{\eta^2}{K} - \frac{\eta}{2(1-\beta)} \mathbb{E} \|\nabla F(\mathbf{w}_t)\|^2. \end{aligned}$$

$$\mathbb{E} \|\nabla F(\mathbf{w}_t)\|^2 \leq \frac{2(1-\beta)[\mathbb{E}F(\bar{\mathbf{z}}_t) - \mathbb{E}F(\bar{\mathbf{z}}_{t+1})]}{\eta} + \frac{L\sigma^2}{(1-\beta)b} \frac{\eta}{K} + (8C_2 + 10\lambda^2 E^2)L^2 \eta^2.$$

Summing up the above equation from $t = 0$ to $T - 1$, we have

$$\frac{1}{T} \sum_{t \in [T]} \mathbb{E} \|\nabla F(\mathbf{w}_t)\|^2 \leq \frac{2(1-\beta)(F(\bar{\mathbf{z}}_0) - F^*)}{T\eta} + \frac{L\sigma^2}{(1-\beta)b} \frac{\eta}{K} + (8C_2 + 10\lambda^2 E^2)L^2 \eta^2.$$

References

Alham Fikri Aji and Kenneth Heafield. Sparse communication for distributed gradient descent. In *Proceedings of the Conference on Empirical Methods in Natural Language Processing*, pages 440–445, 2017.

- Dan Alistarh, Demjan Grubic, Jerry Li, Ryota Tomioka, and Milan Vojnovic. QSGD: Communication-efficient SGD via gradient quantization and encoding. In *Advances in Neural Information Processing Systems*, pages 1707–1718, 2017.
- Dan Alistarh, Torsten Hoefer, Mikael Johansson, Nikola Konstantinov, Sarit Khirirat, and Cédric Renggli. The convergence of sparsified gradient methods. In *Advances in Neural Information Processing Systems*, pages 5977–5987, 2018.
- Debraj Basu, Deepesh Data, Can Karakus, and Suhas N. Diggavi. Qsparse-local-sgd: Distributed SGD with quantization, sparsification and local computations. In *Advances in Neural Information Processing Systems*, pages 14668–14679, 2019.
- Léon Bottou. Large-scale machine learning with stochastic gradient descent. In *Proceedings of the International Conference on Computational Statistics*, pages 177–186, 2010.
- Tom Brown, Benjamin Mann, Nick Ryder, Melanie Subbiah, Jared D Kaplan, Prafulla Dhariwal, Arvind Neelakantan, Pranav Shyam, Girish Sastry, Amanda Askell, et al. Language models are few-shot learners. In *Advances in Neural Information Processing Systems*, pages 1877–1901, 2020.
- Jacob Devlin, Ming-Wei Chang, Kenton Lee, and Kristina Toutanova. Bert: Pre-training of deep bidirectional transformers for language understanding. In *Proceedings of the Conference of the North American Chapter of the Association for Computational Linguistics: Human Language Technologies*, pages 4171–4186, 2019.
- Kaiming He, Xiangyu Zhang, Shaoqing Ren, and Jian Sun. Deep residual learning for image recognition. In *Proceedings of the IEEE/CVF Conference on Computer Vision and Pattern Recognition*, pages 770–778, 2016.
- Kevin Hsieh, Amar Phanishayee, Onur Mutlu, and Phillip B. Gibbons. The non-iid data quagmire of decentralized machine learning. In *Proceedings of the International Conference on Machine Learning*, pages 4387–4398, 2020.
- Tzu-Ming Harry Hsu, Hang Qi, and Matthew Brown. Measuring the effects of non-identical data distribution for federated visual classification. *CoRR*, abs/1909.06335, 2019.
- Peng Jiang and Gagan Agrawal. A linear speedup analysis of distributed deep learning with sparse and quantized communication. In *Advances in Neural Information Processing Systems*, pages 2530–2541, 2018.
- Rie Johnson and Tong Zhang. Accelerating stochastic gradient descent using predictive variance reduction. In *Advances in Neural Information Processing Systems*, pages 315–323, 2013.
- Sai Praneeth Karimireddy, Quentin Rebjock, Sebastian U. Stich, and Martin Jaggi. Error feedback fixes signsgd and other gradient compression schemes. In *Proceedings of International Conference on Machine Learning*, pages 3252–3261, 2019.
- Diederik P. Kingma and Jimmy Ba. Adam: A method for stochastic optimization. In *Proceedings of International Conference on Learning Representations*, 2015.

- Anastasia Koloskova, Tao Lin, Sebastian U Stich, and Martin Jaggi. Decentralized deep learning with arbitrary communication compression. In *Proceedings of International Conference on Learning Representations*, 2020.
- Alex Krizhevsky, Ilya Sutskever, and Geoffrey E. Hinton. Imagenet classification with deep convolutional neural networks. In *Advances in Neural Information Processing Systems*, pages 1106–1114, 2012.
- Guanghui Lan. An optimal method for stochastic composite optimization. *Mathematical Programming*, 133(1-2):365–397, 2012.
- Seung Hoon Lee, Seunghyun Lee, and Byung Cheol Song. Vision transformer for small-size datasets. *CoRR*, abs/2112.13492, 2021.
- Mu Li, David G. Andersen, Jun Woo Park, Alexander J. Smola, Amr Ahmed, Vanja Josifovski, James Long, Eugene J. Shekita, and Bor-Yiing Su. Scaling distributed machine learning with the parameter server. In *Proceedings of the 11th Symposium on Operating Systems Design and Implementation*, pages 583–598, 2014.
- Tao Lin, Sai Praneeth Karimireddy, Sebastian U. Stich, and Martin Jaggi. Quasi-global momentum: Accelerating decentralized deep learning on heterogeneous data. In *Proceedings of International Conference on Machine Learning*, pages 6654–6665, 2021.
- Yujun Lin, Song Han, Huizi Mao, Yu Wang, and Bill Dally. Deep gradient compression: Reducing the communication bandwidth for distributed training. In *Proceedings of International Conference on Learning Representations*, 2018.
- Ilya Loshchilov and Frank Hutter. SGDR: Stochastic gradient descent with warm restarts. In *Proceedings of International Conference on Learning Representations*, 2017.
- Boris Polyak. Some methods of speeding up the convergence of iteration methods. *Ussr Computational Mathematics and Mathematical Physics*, 4:1–17, 12 1964.
- Herbert Robbins and Sutton Monro. A stochastic approximation method. *Annals of Mathematical Statistics*, 22:400–407, 1951.
- Sebastian U. Stich, Jean-Baptiste Cordonnier, and Martin Jaggi. Sparsified SGD with memory. In *Advances in Neural Information Processing Systems*, pages 4452–4463, 2018.
- Ilya Sutskever, James Martens, George E. Dahl, and Geoffrey E. Hinton. On the importance of initialization and momentum in deep learning. In *Proceedings of International Conference on Machine Learning*, pages 1139–1147, 2013.
- Hanlin Tang, Chen Yu, Xiangru Lian, Tong Zhang, and Ji Liu. Doublesqueeze: Parallel stochastic gradient descent with double-pass error-compensated compression. In *Proceedings of International Conference on Machine Learning*, pages 6155–6165, 2019.
- Hugo Touvron, Thibaut Lavril, Gautier Izacard, Xavier Martinet, Marie-Anne Lachaux, Timothée Lacroix, Baptiste Rozière, Naman Goyal, Eric Hambro, Faisal Azhar, Aurélien Rodriguez, Armand Joulin, Edouard Grave, and Guillaume Lample. Llama: Open and efficient foundation language models. *CoRR*, abs/2302.13971, 2023.

- Paul Tseng. An incremental gradient(-projection) method with momentum term and adaptive stepsize rule. *SIAM Journal on Optimization*, 8(2):506–531, 1998.
- Thijs Vogels, Sai Praneeth Karimireddy, and Martin Jaggi. Powersgd: Practical low-rank gradient compression for distributed optimization. In *Advances in Neural Information Processing Systems*, 2019.
- Wei Wen, Cong Xu, Feng Yan, Chunpeng Wu, Yandan Wang, Yiran Chen, and Hai Li. Terngrad: Ternary gradients to reduce communication in distributed deep learning. In *Advances in Neural Information Processing Systems*, pages 1508–1518, 2017.
- Yuxin Wu and Kaiming He. Group normalization. In *Proceedings of the European Conference on Computer Vision*, pages 3–19, 2018.
- Cong Xie, Shuai Zheng, Oluwasanmi Koyejo, Indranil Gupta, Mu Li, and Haibin Lin. CSER: Communication-efficient SGD with error reset. In *Advances in Neural Information Processing Systems*, pages 12593–12603, 2020.
- An Xu and Heng Huang. Detached error feedback for distributed SGD with random sparsification. In *Proceedings of International Conference on Machine Learning*, pages 24550–24575, 2022.
- Shen-Yi Zhao, Gong-Duo Zhang, Ming-Wei Li, and Wu-Jun Li. Proximal scope for distributed sparse learning. In *Advances in Neural Information Processing Systems*, 2018.
- Shen-Yi Zhao, Yin-Peng Xie, and Wu-Jun Li. Stochastic normalized gradient descent with momentum for large batch training. *CoRR*, abs/2007.13985, 2020.
- Shen-Yi Zhao, Yin-Peng Xie, and Wu-Jun Li. On the convergence and improvement of stochastic normalized gradient descent. *Sci. China Inf. Sci.*, 64(3), 2021.